

Effects of Mountain Uplift and Climatic Oscillations on Phylogeography and Species Divergence of Notholirion (Liliaceae)

Rui-Yu Cheng¹, Juan Li¹, Deng-Feng Xie¹, renxiu zhou¹, Qing Li², Yanglina Yu², Xingjin He¹, and Songdong Zhou¹

¹Sichuan University

²Chengdu Branch of Giant Panda National Park

March 10, 2024

Abstract

Exploring the geological events and climate change in the Himalaya-Hengduan Mountains (HHM) region and the Qinghai-Tibet Plateau (QTP) is crucial for understanding the impact of environmental change on biogeographic distribution and biological evolution. To delve deeper into these mechanisms, we reconstructed the evolutionary history of three Notholirion species that span these regions. Here, we examined a total of 254 individuals from 31 populations of these three species, utilizing five chloroplast DNA (cpDNA) (*matK*, *ndhA*, *ndhG-ndhI*, *petB-petD*, and *petL-petG*), along with one nuclear DNA region (internal transcribed spacer, *ITS*). We identified 14 haplotypes from cpDNA and 27 haplotypes from the *ITS*, each specific to corresponding species. Robust haplotype trees were detected, and obvious discrepancies were found between the cpDNA and *ITS* trees. A total of 147 chloroplast genomes were used for divergence time estimation, of which 10 chloroplast genomes from distinct populations of Notholirion species provided a comprehensive representation of the genus. The divergence time estimation results suggested that species of Notholirion genus originated in the southern Himalayan region during the Late Oligocene period (25.05 Ma), and the three Notholirion species then diverged during the Late Pliocene period (7.43 Ma). Our maximum model forecasts that the overall distribution range of Notholirion over four different periods remains relatively stable, from LIG to the future. The origin of the genus Notholirion was triggered by sustained climate fluctuations during the Late Oligocene, with the uplift of the Himalayas and the subsequent orogenic movements intensifying climate changes and further promoting the species divergence of Notholirion. A long evolutionary history, coupled with sexual reproduction and habitat fragmentation, likely contributed to the higher genetic diversity of Notholirion. The higher genetic differentiation among Notholirion populations may be attributed to drastic changes in the external environment within their range, as well as their constrained capacity for seed production and dispersal.

1 Introduction

The Qinghai-Tibet Plateau (QTP), as the "roof of the world", has fostered a variety of plateau organisms, and the Himalayan-Hengduan Mountains (HHM) on *ITS* margin represent two distinct biodiversity hotspots (Deng, Ding, & Deng, 2015; Favre et al., 2015; H. H. Meng et al., 2017). As key features of the biodiversity hotspots of East and South Asia, Himalaya Mountains define the southern edge of the QTP, whereas the Hengduan Mountains of Southwest China form the southeastern frontier of the plateau (Marchese, 2015; Y. L. Zhang, Li, & Zheng, 2002). Both regions have impressive animal and plant diversity, with alpine plant diversity being an important contributor to the hotspot (D. Z. Li, 2008; J. Li et al., 2020; C. Xie et al., 2019). Previous studies have suggested that the Himalayas were formed by the collision of the Indo-Australian plate with Eurasian plate, accompanied by continuous and prolonged uplifts (Aitchison & Ali, 2008; Dupont-Nivet, Lippert, Hinsbergen, Meijers, & Kapp, 2010; H. B. Zheng, Powell, An, Zhou, & Dong, 2000). The collision of the Indian plate and Eurasia resulted in the consequent rise of the Himalayas and QTP. This collision also created folded mountains and faulted basins that formed the present-day HHM (Chatterjee, Goswami,

& Scotese, 2013; Dupont-Nivet et al., 2010). Most studies suggest that the collision began in the Eocene, around 55-50 Mya, followed by a continuous uplift of the Himalayas. parts of the region, such as Thakkhola, Gyirong and Zhada, reached an average elevation of about 4000 to 6000 m during the Miocene (Chatterjee et al., 2013; Dupont-Nivet et al., 2010; Saylor et al., 2009; Q. Zhang & Willems, 2012). During the Late Miocene and the Pliocene, the QTP experienced further uplift. The uplift of the HHM on the southeastern edge of the QTP was particularly pronounced and reached *ITS* peak elevation rapidly before the Late Pliocene (Mulch & Chamberlain, 2006; Xiong et al., 2022; H. B. Zheng et al., 2000).

The formation and uplift of the QTP have had a profound impact on the local area and *ITS* surrounding regions. This has resulted in a series of topographic and climatic changes, which has especially shaped the unusually rugged and complex topography of the HHM and the special East Asian monsoon climate of this region (Cao, Shi, Zhang, & Wang, 2009; Huntington, Blythe, & Hodges, 2006; X. Sun & Wang, 2005; P. Z. Zhang et al., 2004). Since the Quaternary period, climatic fluctuations have had significant effects on the distribution and history of plants populations in the Northern Hemisphere, causing their range-wide migration or extinction and possibly driving local adaptation (J. M. Chen, Zhi-Yuan, Yuan, & Wang, 2014; G. M. Hewitt, 2004; Hickerson et al., 2010). Previous studies have shown that there were four major ice ages and three interglacials that occurred during the Pleistocene, with each ice period being separated by interglacial period. The repeated alternation of ice ages and interglacials caused oscillations of warm and cold climates, which profoundly affected the genetic diversity and spatial distribution patterns of biological taxa found on the QTP and adjacent areas (Borns, 1994; G. Hewitt, 2000; Keller & Seehausen, 2012; Z. Zhang & Sun, 2011). And the repeated alternating cycles of population contraction during the ice age and expansion after the ice age became the dominant pattern for many plants in the Northern Hemisphere, enabling their survival throughout the Quaternary ice age (Godfrey M. Hewitt, 1996). On the QTP and *ITS* adjacent areas, the HHM region in the southeastern part of the QTP may have served as an important refuge for endemic species during the ice age, thanks to *ITS* distinctive mountainous topography (Q. B. Gao et al., 2012; J. Q. Liu, Duan, Hao, XuemgUn, & Sun, 2014; Qiu, Fu, & Comes, 2011). This region is characterized by north-south peaks separated by valley bottoms (Song et al., 2016). From valleys situated approximately 1,000 m above sea level to the peak of Minya Konka at 7,556 m, the huge drop in altitude can form “sky islands” (Kai & Jiang, 2014; Qian, Ricklefs, & Thuiller, 2021). During the Quaternary, these low elevation valley areas on the edge of the ice age impact may have provided shelter for certain local plants to survive the ice age (Q. B. Gao et al., 2012; J. Q. Liu et al., 2014). In addition, many studies have suggested that during the Ice Age, plant species from the QTP region may have survived in invisible refuges at high altitudes (J. Q. Liu, Sun, Ge, Gao, & Qiu, 2012; Luo, Yue, & Sun, 2016). These different habitat zones and ecosystems, such as the refuges found in different elevation zones and sky islands, have also resulted in speciation and radiation (J. Q. Liu et al., 2014; Qiu et al., 2011; H. Wang et al., 2010; Xu et al., 2010). Thus, the climatic and specific topographic changes caused by the uplift of the QTP have played a key role in the origin, speciation and evolution of several plant taxa throughout the HHM and adjacent areas.

The HHM region has a special climatic environment, complex geological landscape, and bioecological diversity, making it an ideal and captivating location for studying species diversification and adaptive evolution. Previous studies have mostly focused on how species in the HHM adapt to climatic oscillations brought by uplift of the plateau (Luo et al., 2016; Shahzad, Jia, Chen, Zeb, & Li, 2017; Xu et al., 2010; J. Yang, Zhou, Huang, & He, 2018). The refuge pattern of species in the QTP region during the ice age, as well as their migration out of the plateau, is also a topic of current research (Q. Li et al., 2020; H. R. Liu et al., 2022; M. L. Liu, He, López-Pujol, Jia, & Li, 2019; Shahzad et al., 2017). Available phylogenetic and biogeographic studies have suggested that population differentiation and demography within species have also been strongly influenced by the uplift of the QTP and the consequent climate oscillations during the Quaternary ice age in the region (H. R. Liu et al., 2022; Y. Sun et al., 2014; H. Wang et al., 2010; F. S. Yang, Qin, Li, & Wang, 2012). In recent years, while most studies continue to focus on population differentiation and biogeography within species, very few researchers have focused on an entire endemic genus in the HHM region (H. Y. Zheng, Guo, Price, He, & Zhou, 2021). Therefore, we expect to investigate the origins, diversification, and population response of species to climatic oscillations since the Pleistocene by studying the distribution and

population history of plant taxa that are mainly distributed in the HHM and QTP region.

Notholirion is a genus of Liliaceae and is mainly distributed in the HHM and QTP region, where it grows in alpine meadows and shrublands (M. Yang, Zhou, Xingjin, & Peng, 2016). *Notholirion* species are distinguished from other genera of Liliaceae by the presence of racemes and numerous small bulbs surrounding their bulbs. According to the records of *Notholirion* in the Flora of China and Li et al. (2021), four morphologically distinct species are accepted, and three species occur in the HHM and QTP region, except for *N. koeiei*, which are found in Iran and Iraq in the West Asia region (J. Li et al., 2022; J. Q. Liu et al., 2014). Particularly, the two species with distribution in China (*N. macrophyllum* and *N. bulbuliferum*) both live at altitudes above 2800 m and are typical plants of the QTP (M. Yang et al., 2016). *N. bulbuliferum* exhibits the widest distribution in China, ranging from the Qinling Mountains in Shaanxi to Western Sichuan, northwestern Yunnan, and eastern Tibet. *N. macrophyllum* is restricted to specific areas such as Jilong in Tibet and Daocheng in Sichuan (J. Li et al., 2022). Additionally, we were fortunate to acquire a population of *N. thomsonianum* from Nepal. *N. thomsonianum* does not occur naturally in China, but to maximize the representation of *Notholirion* species, we included the only available population from Nepal in our analysis. As for *N. koeiei*, there are only five recorded specimens from Iraq and Iran in western Asia, and unfortunately, we did not have access to any samples of this species. Based on the descriptions in the Flora of China and our own field observations, we have noted several distinct characteristics among the *Notholirion* species. Mature plants of *N. macrophyllum* typically have a height of less than 40 cm, and their racemes typically bear 3-7 flowers. On the other hand, *N. bulbuliferum* and *N. thomsonianum* generally grow taller than 40 cm, and their racemes typically bear a larger number of flowers. Furthermore, *N. bulbuliferum* lacks any stripes at the base of the tepals and typically flowers from July to August, whereas *N. thomsonianum* exhibits longitudinal dark stripes consisting of spots at the base of the tepals and flowers from March to May (S. C. Chen, Liang, Xu, & Minoru, 2000; J. Li et al., 2022). The recent phylogenetic study indicated that *N. bulbuliferum* and *N. macrophyllum* are sister taxa, and they form a sister clade together with *N. thomsonianum*. The three *Notholirion* species form a distinct monophyletic clade. Therefore, this genus is an ideal taxon to investigate the evolution and diversification of alpine plants in the HHM and QTP region (J. Li et al., 2022).

In this study, we reconstructed the phylogenetic tree of *Notholirion* based on data from 31 populations of three species that distributed in the HHM and QTP regions. We used biogeographical and population genetics approaches to identify the mechanism of origin, genetic structure, and lineage evolutionary history in the genus *Notholirion*. Our aims were to: (i) reconstruct the phylogenetic relationships within the genus *Notholirion* using materials from 31 populations; (ii) investigate the origin and species diversification of *Notholirion* in the HHM and QTP regions; (iii) explore the geological and climatic changes that influenced distribution shifts and genetic diversity of *Notholirion*. We hope that this study will provide some clues to explore the evolutionary patterns of species in the HHM region.

2 Materials and Methods

2.1 Sample collection

To observe as much variation of the species as possible in the wild, a total of 254 individuals belonging to three species of *Notholirion* were collected based on our field explorations and past herbarium records. These individuals were from 31 populations at elevations above 2800 m in Nepal, Tibet (Xizang), Sichuan and Yunnan provinces (**Figure 1 and Supplementary Table 1**). Sampling localities covered almost the entire distribution of the three species and 6 to 10 individuals were randomly sampled from each population with at least 20 m between the collected samples. Fresh leaves were collected and dried immediately with silica gel. The voucher specimens were deposited at Sichuan University Herbarium (SZ).

2.2 DNA Extraction, PCR Amplification, and Sequencing

Total genomic DNA was extracted from dried leaf tissue using a modified cetyltrimethylammonium bromide (CTAB) protocol (E. & C., 1980). Raw data of the 10 newly sequenced whole plastid genomes from *Notholirion* species were generated by Illumina platform, generating 150 bp paired-end reads at Novogene (Beijing, China). The reads were assembled using the program NOVOPlasty v2.6.2 (Dierckxsens, Mardulyn,

& Smits, 2017) and the genome annotation was performed using Plastid Genome Annotator (PGA)(Qu, Moore, Li, & Yi, 2019). Manual adjustment compared with related species' plastomes was conducted in Geneious v9.0.2(Kearse et al., 2012). For the plastid DNA (cpDNA) fragment, we designed 15 primer pairs using the whole plastid genome of *Notholirion*(GenBank accessions NC046464, MH011354) and finally got five chloroplast fragments (*matK* , *ndhA* , *ndhG-I* , *petB-D* and *petL-G*) for analysis. We amplified and sequenced *ITS*(*ITS1-5.8sRNA-ITS2*)(White, Bruns, Lee, & Taylor, 1990) and the five chloroplast fragments above at Sangon Biotech Co. Ltd. (Chengdu, China) and all DNA fragments were aligned and manually adjusted using the software MEGA X(Kumar, Stecher, Li, Knyaz, & Tamura, 2018).

2.3 Phylogenetic analyses

The phylogeny reconstruction based on two databases of haplotypes (*ITS* and cpDNA sequences) were performed using Bayesian inference (BI) and maximum likelihood (ML). Gaps were treated as missing data during the tree searches. The two programs MrBayes version 3.2(Ronquist et al., 2012) and RAxML v.8(Stamatakis, 2014) were used to conduct BI and ML analyses. The best model for *ITS* and cpDNA were both GTR+G (BI and ML) inferred by ModelFinder(Kalyaanamoorthy, Minh, Wong, von Haeseler, & Jermin, 2017) based on the Akaike information criterion (AIC). Markov chain Monte Carlo (MCMC) method was used for BI and set to run 10 million generations, sample every 1,000 generations, discard 25% of the trees as burn-in. The convergence of MCMC inference was evaluated using Tracer v.1.7.11 to ensure sufficient samples (ESS > 200) by checking the ESS (Effective Sample Size) value. Besides, we ran RAxML on *ITS* and cpDNA with 1000 bootstrap replicates. Finally, BI posterior probabilities (BI PP) and ML bootstrap support (ML BS) were presented at the nodes separately.

2.4 Divergence Time Estimate

There are currently no well-documented fossils in Liliaceae, and thus fossil constraints were limited to Liliales. We used 10 populations of *Notholirion* plastomes and 137 other plastomes to calibrate the divergence time of *Notholirion* (**Supplementary Table 2**) . Referring to previous studies(H. T. Li et al., 2019; J. Li et al., 2022; D. F. Xie et al., 2020) and to minimize the effects of missing data, we only used combined single-copy CDS genes data set derived from 147 plastomes for the estimation of divergence time. The common CDS of 147 plastomes were extracted, respectively aligned, and then concatenated as the plastome CDS dataset, using PhyloSuite v1.2.2(D. Zhang et al., 2020). Estimations of divergence time were performed using an uncorrelated lognormal relaxed molecular clock method implemented in the BEAST 1.10.4 program(Suchard et al., 2018). BEAUti was used to set criteria for analyses where we used a GTR + G substitution model selected by ModelFinder and a Yule process(Gernhard, 2008). An optimal partitioning scheme was determined using the PartitionFinder 2 program(Lanfear, Frandsen, Wright, Senfeld, & Calcott, 2017) and six calibration points were used to calibrate time (**Supplementary Table 3**) . MCMC analyses were run for 100 million generations with parameters sampled every 10,000 generations after discarding the first 10% of generations as burnin. The convergence of the stationary distribution was accessed by ESS values (>200) using the Tracer v.1.7.11. Maximum clade credibility (MCC) trees were produced using TreeAnnotator v1.8.4(Helfrich, Rieb, Abrami, Lücking, & Mehler, 2018) and visualized in FigTree v1.4.2(Rambaut, 2014).

2.5 Ancestral Area Reconstruction

To explore the biogeographic history of *Notholirion* plants, we used three regions based on the paleogeographic and climatic evidence, geographic distribution and floral composition throughout the Himalayas-Hengduan Mountains (HHM) for ancestral area reconstruction(Buerki et al., 2012; Tu, Volis, Dillon, Sun, & Wen, 2010; H. Y. Zheng et al., 2021): (A) southern Himalayas, (B) eastern Himalayas, (C) Hengduan Mountains. The Statistical Dispersal-Vicariance (S-DIVA) analysis as implemented in the RASP v4(Y. Yu, Blair, & He, 2020) was used for the reconstruction. We used the BI tree based on the cpDNA datasets (obtained by phylogenetic analyses) for the S-DIVA analyses. The uncertainty in the root areas of an outgroup can lead to biased inferences for the crown node of the ingroups(Y. Yu, Harris, Blair, & He, 2015), outgroups were removed before ancestral-state reconstruction. To explore the effects of area constraints, the maximum

number of areas at each node was set to two.

2.6 Population Genetics, Phylogeographic Analyses, and Demographic History

All the DNA sequences were edited by SeqMan (DNASTar package; DNASTar Inc., Madison, WI, United States) to obtain consensus sequences. The program MAFFT v.7.369b(Katoh & Standley, 2013) was used to align for subsequent manual adjustments. Haplotype diversity (H_d)(Nei & Tajima, 1981) and nucleotide diversity (π)(Nei & Li, 1979) for each population were calculated using DNAsp v6.0(Rozas et al., 2017) to verify the degrees and patterns of diversity. The haplotypes of the two gene fragment datasets and the distribution of all haplotypes on the map were then plotted separately in the software PopART using the Minimum spanning method(Bandelt, Forster, & Röhl, 1999). PERMUT was used to access the total diversity (H_T), within-population diversity (H_S) and population differentiation indices (G_{ST} and N_{ST})(Pons & Petit, 1996). And a U-statistic was used to test the phylogeographic structure by comparing G_{ST} and N_{ST} . In addition, analyses of molecular variance (AMOVA) was performed using ARLEQUIN v3.5(Excoffier & Lischer, 2010) to assess the genetic differentiation within and between populations, and 1000 random permutations were conducted to test the significance of partitioning. To detect whether the populations in *Notholirion* experienced a recent population expansion, a mismatch distribution analysis (MDA)(Schneider & Excoffier, 1999) was carried out using the ARLEQUIN v3.5(Excoffier & Lischer, 2010). Additionally, Neutrality test (Fu's F_s ; Tajima's D)(Tajima, 1989) was also conducted to test whether there was potential population expansion in *Notholirion* using DnaSP v6.0 program. The smoothness of observed mismatch distribution was detected by calculating the Harpending's raggedness index (H_{rag})(Schneider & Excoffier, 1999) and the sum of squared deviations (SSD) between observed and expected mismatch distributions.

2.7 Species Distribution Modeling

MAXENT 3.3.3e(Phillips, Anderson, & Schapire, 2006) was used to predict the distribution of *Notholirion* in China during 4 time periods: Last Interglacial (LIG), Last Glacial Maximum (LGM), and the present and future. The samples collected in this study covered the distribution of all 30 populations of the genus *Notholirion* throughout China for which specimens were recorded. Nineteen bioclimatic environment variables(Alemu & Wimberly, 2020) from four time periods above were downloaded from the WorldClim database(Fick & Hijmans, 2017) and employed in modeling analyses. In MAXENT, due to the small sample size of our data (15–79 localities), only the linear + quadratic + hinge functional forms were used. Here, models were built using linear + quadratic + hinge features, random training data was set to 25%, repeat run type was set to Subsample, maximum iterations were set to 1000, and other parameters were set by default. We also calculated the area under the Receiver Operating Characteristic (ROC)(Fawcett, 2005) and Operating Characteristic Curve (AUC)(Ellis, Yahr, Belinchón, & Coppins, 2014) to observe the accuracy of each model prediction. Usually, good model performance was assessed by AUC values above 0.7(Elith & Leathwick, 2009; Fielding, 1997; Peterson, Pape, & Soberón., 2008). The spatial distribution range map of the final modeling results was plotted by the software DIVA-GIS v 7.5(Hijmans, Cameron, Parra, Jones, & Jarvis, 2010).

3 Results

3.1 Genetic Diversity and Structure

ITS and five chloroplast fragments (*matK*, *ndhA*, *ndhG-I*, *petB-D*, *petL-G*) were used to analyze 254 individuals from 31 populations of the nine *Notholirion* species. The *ITS* and cpDNA haplotype frequencies of each population are listed in **Supplementary Table 4**, and the geographical distributions of haplotypes are shown in **Figures 2, 4**. The length of *ITS* sequence we used in this study was 671 bp containing 60 polymorphic sites. We detected 27 *ITS* haplotypes (N1–N27), which were species-specific as none were shared by any two species (**Figure 3**). Most of the populations have only one or two haplotypes and populations with more than three haplotypes only occurred in *N. bulbuliferum*. Besides, the total length of the aligned sequences of cpDNA was 2753 bp containing 39 polymorphic sites were recovered with 14 haplotypes. Like *ITS* haplotypes, all cpDNA haplotypes were species-specific in *Notholirion* (**Figure 5**). All the populations have only one or two haplotypes, with only 22.58% of the populations having two

haplotypes.

The haplotype diversity (H_d) of *ITS* ranged from 0.000 to 0.867, and nucleotide diversity (π) ranged from 0.000 to 0.011 across all species (**Supplementary Table 4**). Total gene diversity (H_T) value was all higher than the average gene diversity within populations (H_S) at the level of species and genus. Additionally, the number of substitution types (N_{ST}) was higher than interpopulation differentiation (G_{ST}), which indicated that a significant phylogeographic structure existed in *Notholirion* (Table 1). The haplotype diversity (H_d) of cpDNA ranged from 0.000 to 0.800, and nucleotide diversity (π) ranged from 0.000 to 0.004 across all species (**Supplementary Table 4**). Like *ITS* haplotypes, the total gene diversity (H_T) value was higher than the average gene diversity within populations (H_S), whether at the level of species or genus. Total NST was significantly higher than GST, indicating significant phylogeographic structure in *Notholirion* (**Table 1**).

ITS AMOVA revealed that the primary genetic variation (74.86% - 98.68%) in *N. bulbuliferum* and *N. macrophyllum* occurred among populations (**Table 2**). Furthermore, the AMOVA analysis of cpDNA data indicated a genetic differentiation pattern similar to that of *ITS*, with 93.73% - 98.85% of the total variation distributed among populations (**Table 2**).

Table 1 Genetic diversity and genetic differentiation of three species within *Notholirion* based on cpDNA and *ITS*.

Species	H_S	H_T	G_{ST}	N_{ST}
nrDNA				
<i>N. bulbuliferum</i>	0.199 (0.0611)	0.750 (0.0711)	0.705 (0.0741)	0.716 (0.0781)
<i>N. macrophyllum</i>	0.156 (0.1556)	0.667 (0.3156)	0.767 (NC)	0.986 (NC)
<i>N. thomsonianum</i>	-	-	-	-
Total	0.227 (0.0617)	0.796 (0.0623)	0.715 (0.0705)	0.767 (0.0899)
cpDNA				
<i>N. bulbuliferum</i>	0.107 (0.0395)	0.766 (0.0529)	0.860 (0.0476)	0.907 (0.0369)
<i>N. macrophyllum</i>	0.119 (0.1185)	0.667 (0.2933)	0.822 (NC)	0.983 (NC)
<i>N. thomsonianum</i>	-	-	-	-
Total	0.677 (0.0600)	0.931 (0.0080)	0.273 (0.0640)	0.402 (0.1710)

Table2 Analysis of molecular variance (AMOVA) based on the cpDNA and nrDNA

	Source of variation	d.f.	SS	VC	PV (%)	Fixation Indices
ITS	ITS	ITS	ITS	ITS	ITS	ITS
All species	Among species	1	195.447	5.12027	70.37	FSC: 0.79869
	Among populations within species					
	Within populations	27	383.922	1.72216	23.67	FST: 0.94035
		205	88.986	0.43408	5.97	FCT: 0.70367
<i>N. bulbuliferum</i>	Among populations	26	296.338	1.37585	74.86	FST: 0.74856

	Source of variation	d.f.	SS	VC	PV (%)	Fixation Indices
<i>N. macrophyllum</i>	Within populations	188	86.886	0.46216	25.14	
	Among populations	1	87.584	9.23196	98.68	FST: 0.98680
	Within populations	17	2.100	0.12353	1.32	
<i>N. thomsonianum</i>	Among populations	-	-	-	-	-
	Within populations	-	-	-	-	-
All samples	Among populations	30	1060.215	4.27072	91.45	FST: 0.91455
	Within populations	223	88.986	0.39904	8.55	
cpDNA	cpDNA	cpDNA	cpDNA	cpDNA	cpDNA	cpDNA
All species	Among species	1	166.421	3.18145	76.19	FSC: 0.95113
	Among populations within species					
	Within populations	28	214.406	0.94567	22.65	FST: 0.98836
<i>N. bulbiferum</i>	Among populations	213	10.350	0.04859	1.16	FCT: 0.76189
	Within populations	26	156.485	0.75095	93.73	FST: 0.93726
	Within populations	188	9.450	0.05027	6.27	
<i>N. macrophyllum</i>	Among populations	2	57.921	3.10303	98.85	FST: 0.98853
	Within populations	25	0.900	0.03600	1.15	
<i>N. thomsonianum</i>	Among populations	-	-	-	-	-
	Within populations	-	-	-	-	-
All samples	Among populations	30	569.516	2.32391	98.03	FST: 0.98033
	Within populations	222	10.350	0.04662	1.97	

Notes: FCT = differentiation among groups; FST = differentiation among populations; FSC = differentiation among populations within groups. ** P < 0.001.

3.2 Phylogeny Reconstruction

The ML and BI topologies of *ITS* and cpDNA haplotype phylogenetic trees were consistent on branches with strong support (**Figure 6**). Partial inconsistencies between the *ITS* and cpDNA trees occurred regarding

the phylogenetic relationships of *N. bulbuliferum* and *N. macrophyllum*. In the *ITS* haplotype phylogenetic trees, *N. bulbuliferum* and *N. macrophyllum* each had a haplotype (N7 and N26) embedded in the branch of the other (**Figure 6a**). In the cpDNA haplotype phylogenetic trees, the haplotypes of all species are well clustered into a single branch, forming a good monophyletic clade (**Figure 6b**). Overall, no haplotypes were shared among the three *Notholirion* species, and each species in general formed *ITS* own individual branch in the *ITS* and cpDNA trees. The *ITS* haplotype network map and the *ITS* haplotype phylogenetic tree constructed by TCS network were consistent, with *N. bulbuliferum* and *N. macrophyllum* each having a haplotype (N7 and N26) embedded in the branch of the other (**Figure 3**). While in cpDNA, the haplotype network map and haplotype phylogenetic tree were consistent, with each of the three species forming a separate monophyletic (**Figure 5**).

3.3 Divergence Time Estimation

As we all know, the molecular markers of chloroplast are closer to neutral and have matrilineal genetic stability and widely used in the process of divergence time estimation and biogeographic deduction. We finally selected the results obtained based on common CDS for the subsequent elaboration of the differentiation history of *Notholirion*. According to the beast-derived age estimate based on the common CDS of 147 plastid genomes and 4 fossil calibration sites, the crown age of *Notholirion* was dated to be 25.05 Ma (95% HPD:35.56-16.62 Ma). The divergence times of *N. thomsonianum* was estimated at 7.43 Ma (95% HPD:14.86-2.53 Ma). And The divergence of *N. macrophyllum* and *N. bulbuliferum* occurred at 2.46 Ma (95% HPD:4.74-0.81 Ma). The results were shown in **Figures 10, 11**.

3.4 Ancestral Area Reconstruction

As the results of ancestral area reconstruction based on cpDNA phylogeny showed, the most recent common ancestor of the *Notholirion* species probably originated in the Southern Himalayas (**region A, blue in the Figure 9, Nodes I**). Meanwhile, the most recent common ancestor of *N. macrophyllum* and *N. bulbuliferum* most likely originated in the Hengduan Mountains (**region C, brown in the Figure 9, Nodes II**). The origin of the genus *Notholirion* is hypothesized to have begun with initial divergence in the Southern Himalayas, followed by migration of a portion of the ancestral taxa to the Eastern Himalayas. From there, some populations continued to migrate and spread eastward to the Hengduan Mountains, where they underwent further divergence.

3.5 Demographic History and Species Distribution Modeling

Based on *ITS* and cpDNA data, we performed mismatch distribution analysis and neutrality test to determine the demographic history of *Notholirion* species. The mismatch distributions graphs for our study species were multimodal and/or very ragged instead of a smooth single-peaked curve, which indicates populations are stable and not shrinking or expanding (**Figure 10**). In addition, the values of Tajima's D and Fu's Fs were non-significant for all *Notholirion* species in the neutrality test, which also means populations have not experienced expansion or sustained growth (**Table 3**).

Considering *Notholirion* and climate scenarios (the LIG, the LGM, the present and the future), the area under the AUC value for the potential climatically suitable areas of *Notholirion* species was high (>0.95), indicating the highest predictive capacity. And the distribution ranges predicted for *Notholirion* species were consistent with the actual geographic distributions. Based on the modeling results, there are slight variations in both the overall distribution range and the optimal distribution range of *Notholirion* across four different periods. The overall distribution range throughout these periods predominantly encompasses the HHM region, while the optimal distribution range (highlighted in red) is mainly concentrated in the Hengduan Mountains and along the margin of the QTP. The suitable distribution area of *Notholirion* on the eastern part of the Tibetan Plateau contracted significantly toward *ITS* eastern edge during the LGM period, and the main best distribution area shifted from the northern part of the Hengduan Mountains to the southern region. And from the LGM period to the present, the distribution area of *Notholirion* re-expands to the eastern part of the Tibetan Plateau. Predictions indicate that the future overall distribution range and optimal distribution area will not significantly differ from the present distribution (**Figure 11**).

Table3 Results of the mismatch distribution analysis and neutrality tests for *Notholirion*

Floras	Tajima's D (p)	Fu's F_s (p)	SSD	H_{rag}
ITS	ITS	ITS	ITS	ITS
<i>N. bulbuliferum</i>	0.07080(0.52800)	-5.26370(0.08000)	0.04602(0.26000)	0.06807(0.41000)
<i>N. macrophyllum</i>	2.86519(0.99500)	12.88345(0.99999)	0.20769(0.01000)	0.34121(0.91000)
<i>N. thomsonianum</i>	-	-	-	-
All	-0.49517(0.32500)	0.55610(0.63000)	0.03180(0.69000)	0.04341(0.43000)
cpDNA	cpDNA	cpDNA	cpDNA	cpDNA
<i>N. bulbuliferum</i>	0.10895(0.54300)	-1.60875(0.33900)	0.01034(0.16000)	0.04323(0.25000)
<i>N. macrophyllum</i>	2.23738(0.95100)	8.15095(0.99999)	0.27275(0.00001)	0.55839(0.99999)
<i>N. thomsonianum</i>	-	-	-	-
All	-0.74429(0.22900)	2.67736(0.79700)	0.03655 (0.08000)	0.07168(0.06000)

4 Discussion

4.1 Genetic Diversity and Structure of *Notholirion*

Biogenetic diversity is the result of the long-term evolution of species and serves as an essential foundation for organisms to adapt to their environment and evolve. It is also a key factor in maintaining the stability and function of ecosystems. The higher the genetic diversity of a species, the better it can adapt to environmental changes. Conversely, when genetic diversity is low, a species is often vulnerable to environmental changes and may lose *ITS* distribution or even become extinct (Soltis & Soltis, 1991; Vranckx, Jacquemyn, Muys, & Honnay, 2012). Previous studies have reported that the average genetic diversity of angiosperms, as inferred from plastid gene data, is 0.67 (Petit et al., 2005). Our analysis of both plastid and *ITS* data sets revealed that the overall genetic diversity (H_T value) of the *Notholirion* was significantly higher than this average (cpDNA: $H_T = 0.931$; *ITS* : $H_T = 0.796$), indicating a remarkably high level of genetic diversity of this group (Table 1). Through a series of analyses of the evolutionary aspects of the origin of the *Notholirion*, we suggested that two factors may have contributed the most to the higher genetic diversity of *Notholirion*: (1) *Notholirion* is the earliest divergent clade of the tribe Lilieae, during the late Oligocene. During *ITS* long evolutionary history, it experienced numerous geological and climatic events such as orogenic movements, monsoonal climatic events, and drought events, which led to the accumulation of a large amount of genetic variation to adapt to environmental changes; (2) *Notholirion* grows at high altitudes with an average altitude of about 3000 meters, mainly in the Himalayan-Hengduan Mountains. The area is influenced by frequent mountain-building movements in the Miocene, resulting in an intricate and complex topography with interlocking rows of high mountain valleys that form the "sky islands". The unique "sky island" environment fragments habitat, leading to alpine plant populations that form relatively isolated and special ecosystems subject to different environmental selection and ecological niche differentiation. This increases the opportunity for genetic drift within populations, which results in a wealth of genetic variation. Thus, the plant taxa distributed in this environment often exhibit a high degree of genetic diversity and unique genotypic assemblages, adapted to the challenges of these extreme environments. Similar results have been found in other plants distributed in the HHM region, such as *Chamaesium* (cpDNA: $H_T = 0.794$; *ITS* : $H_T = 0.718$), *Notopterygium incisum* (cpDNA: $H_T = 0.939$; *ITS* : $H_T = 0.725$) and *Allium* section *Sikkimensia* (cpDNA: $H_T = 0.974$; *ITS* : $H_T = 0.988$) (Shahzad et al., 2017; C. Xie et al., 2019; H. Y. Zheng et al., 2021).

In addition, AMOVA analyses were performed based on both *ITS* and cpDNA datasets. The results showed (Table 2) that if *Notholirion* is considered as a whole, the genetic variation among the 31 populations was large (*ITS* : 91.45%; cpDNA: 98.85%) and within the populations was relatively small (*ITS* : 8.55%; cpDNA: 1.15%), which may be related to the following reasons: (1) field surveys revealed that although *Notholirion* species are distributed in four provinces of southwestern China, they have very specific habitat requirements. Apart from altitude requirements, this genus also necessitates specific heights of companion plants. For instance, *N. macrophyllum* and *N. thomsonianum* prefer to grow in scrub or tall grasses at around 3000m

above sea level, where the plants are roughly the same height as their own height. Hence, almost all populations collected in the field have an extremely limited local distribution, and communication between flora and populations is rare (J. Li et al., 2022); (2) Through our field investigations, we also have observed that *Notholirion* species have very limited seed dispersal ability, and their seed production cycle is quite lengthy. It takes approximately 5 years from seedling to flowering, and after flowering, the primary bulbs of the roots wither, making it impossible for seed production to occur in the following year. Mature seed production is only attainable through newborn seeds and asexual reproduction of small bulbs, which take an additional 5 years to reach the mature stage. This situation with seeds also makes interflora and interpopulation communication very difficult; (3) The genetic differentiation of many plant taxa in the HHM region has been observed to be primarily influenced by the complex geological activities and climate changes that occur in the area. For example, orogenic movements can lead to fragmented habitats, which can reduce gene flow among populations and consequently increase genetic variation among them. Therefore, it is likely that the high genetic differentiation observed among *Notholirion* flora is due to the significant fluctuations in the external environment in the HHM region and *ITS* own specificity. Similar results were found in *Chamaesium*, *Allium* section *Sikkimensia* and *Polygonatum* (Xia et al., 2022; C. Xie et al., 2019; H. Y. Zheng et al., 2021). However, AMOVA results of *N. bulbuliferum* based on *ITS* data showed a lower percentage of genetic variation among *ITS* populations (74.86%) compared to the results based on cpDNA data (93.73). The reason for this inconsistent genetic structure is hypothesized to be as follows: according to the *ITS* data, multiple haplotypes were detected in 27 *N. bulbuliferum* populations, of which N1 was a haplotype common to 15 populations, thus reducing genetic variation among populations.

Both cpDNA and *ITS* datasets showed high levels of haplotype diversity in the haplotype analysis (cpDNA: $Hd = 0.801$; *ITS* : $Hd = 0.788$). There were no shared haplotypes among the three *Notholirion* species, and most haplotypes were restricted to a single population or between several geographically adjacent populations, which is similar to the results found in *Chamaesium* (H. Y. Zheng et al., 2021). We speculate that *Notholirion*, as a high-altitude distributed taxon, has different populations that remain isolated and lack communication with each other during ice ages and interglacial periods. This situation may be due to several environmental factors and the species *ITS* elf, including the inability of high-altitude plants to adapt to low-altitude environments, the fragmentation of habitats in the HHM region, and the formation of unique habitats such as sky islands that make communication between populations difficult, and the long seed production cycle and difficulty of dissemination of *Notholirion* species themselves that limit communication between populations.

4.2 Phylogenetic relationships of *Notholirion*

The phylogenetic analysis using both nuclear gene fragments and plastid fragments confirmed the monophyletic nature of *Notholirion*, which is consistent with previous studies (Huang et al., 2018; Kim & Kim, 2018; J. Li et al., 2022). Within the genus *Notholirion*, the species *N. thomsonianum* was found to be a sister taxon to the branches of *N. macrophyllum* and *N. bulbuliferum*, representing the earliest divergence event as supported by the BEAST divergence time estimates. Notably, some populations showed inconsistencies in their nuclear genetic makeup. The cpDNA tree revealed that all populations of the three *Notholirion* species formed distinct monophyletic branches. However, in the *ITS* tree, two populations of *N. macrophyllum* (MNC and MZT) clustered together with most populations of *N. bulbuliferum*, while *N. bulbuliferum* exhibited a population (BDY) clustered into a single branch with the remaining two populations of *N. macrophyllum*.

The phenomenon of inconsistency between nuclear gene trees and chloroplast gene trees is very common in plant phylogenetic analyses and is typically attributed to convergent evolution, incomplete lineage sorting, hybridization, or gene introgression (Y. Gao, Harris, Li, & Gao, 2020; Y. D. Gao, Harris, & He, 2015; Y. D. Gao, Harris, Zhou, & He, 2013; Huang et al., 2018; X. Liu, Wang, Shao, Ye, & Zhang, 2016). The selected gene fragments in this study are mostly evolutionarily conserved and less influenced by the environment, reducing the likelihood of convergent evolution. Therefore, the main factors considered are incomplete lineage sorting and hybridization. And in many studies on the phylogenetic relationships of plants in the family

Liliaceae, both incomplete lineage sorting and hybridization have been mentioned as factors contributing to conflicts in the phylogenetic relationships (Y. Gao et al., 2020; Y. D. Gao et al., 2015; Y. D. Gao et al., 2013; Huang et al., 2018). Studies have shown that incomplete lineage sorting is more likely to occur when species rapidly expand or have large population sizes (Maddison, 1997). Due to the stochastic nature of the coalescent process, incomplete lineage sorting can lead to random patterns of gene trees among taxa, which may result in inconsistencies between different gene trees (Buckley, Cordeiro, Marshall, & Simon, 2006). Furthermore, lineage sorting in plants generally takes hundreds of millions of years (X. Liu et al., 2016; Pelser et al., 2010). Both *N. macrophyllum* and *N. bulbiferum* are relatively young species that diverged in the last few million years, which is far from reaching the timescale of hundreds of millions of years. Therefore, we speculate that incomplete lineage sorting may be one of the reasons for the observed incongruence between nuclear and chloroplast genomes in *Notholirion*. We know that hybridization plays a significant role in biodiversity and speciation by either reinforcing or disrupting reproductive barriers (Les et al., 2015). Due to the maternal inheritance of organelle genes, gene flow resulting from biparental hybridization is usually manifested only in nuclear genes, leading to inconsistencies between the phylogenetic trees constructed based on nuclear genes and organellar genes (X. Liu et al., 2016). Hybridization is widely observed in the family Liliaceae, as evidenced by numerous reports in wild *Lilium* species and *ITS* frequent use in horticulture for plant breeding purposes (Y. Gao et al., 2020; Y. D. Gao et al., 2015; Y. D. Gao et al., 2013; Pelkonen, Niittyvuopio, Pirttilä, Laine, & Hohtola, 2007). Furthermore, some researchs have suggested that hybridization may be a common phenomenon in Liliaceae plants (Douglas et al., 2011; Muratović, Robin, Bogunić, Šoljan, & Siljak-Yakovlev, 2010). In conclusion, we speculate that incomplete lineage sorting and hybridization may be the primary factors leading to the conflicting phylogenetic trees observed between the nuclear genes and chloroplast genes in *Notholirion*.

4.3 Origin and Diversification of *Notholirion*

In the vast timeline of Earth's evolution, every geological event and climate change has had unprecedented effects on organisms, making it a highly researched topic in the present day. Based on the complete plastid genomic dataset, we estimated the origin of the genus *Notholirion* and the divergence times of the three species within the genus (**Figure 7, 8**). Additionally, we reconstructed their ancestral distribution using the chloroplast fragments (**Figure 9**). The results suggest that the ancestral lineage of the *Notholirion* genus originated in the southern Himalayas during the end of the Tertiary period in the Cenozoic era (25.05 Ma, 95% HPD: 35.56-16.62 Ma). The prevailing theory regarding this period suggests that from 38.0-23.03 Ma, the Earth transitioned from the end of the Eocene epoch through the Oligocene epoch and into the early Miocene epoch. During this time, the climate gradually cooled, resulting in a moderate icehouse climate, and plants and animals evolved and diversified rapidly (O'Brien et al., 2020; Straume, Nummelin, Gaina, & Nisancioglu, 2022). It is during this period that the evolution and spread of modern types of flowering plants primarily took place (Nge, Biffin, Thiele, & Waycott, 2020). Furthermore, during this period, as a result of the gradual collision between the Indian subcontinent and the Eurasian Plate, the Qinghai-Tibetan Plateau continued to uplift both to the south and north. The ongoing uplift of the Qinghai-Tibet Plateau has caused dramatic changes in the topography of the region and has directly contributed to the formation of the monsoon climate (Favre et al., 2015). The significant changes in habitat have also facilitated the formation and differentiation of populations, as seen in *Chamaesium*, *Cardiocrinum*, and *Sinopteris* (J. Li et al., 2022; L. Wang, Yang, Zhang, Zhang, & Zhang, 2023; H. Y. Zheng et al., 2021). Therefore, we speculate that the origin of the genus *Notholirion* is closely related to the uplift events that occurred on Tibetan Plateau.

During the early to middle Miocene (23.03-10 Ma), the Earth's climate experienced significant cooling and entered a period of massive glaciation. The uplift of the Himalayas and surrounding mountains caused aridification of the local climate and a decrease in temperature, limiting plant growth and reproduction and having a profound impact on the evolution of local species, such as *Gentiana crassicaulis*, *Polygonatum* and *Allium* section *Daghestanica* (M. J. Li, Yu, Guo, & He, 2021; Ni, Li, Zhao, Gaawe, & Liu, 2022; Xia et al., 2022). By the late Miocene (10-5.33 Ma), the Qinghai-Tibetan Plateau experienced a more significant uplift and expansion, which affected numerous mountain ranges in the plateau's eastern margin region. Among them, the Himalayas and the Gangdise Mountains run parallel to each other in a northwest-

southeast direction, forming a natural barrier. This allows the warm and humid airflow from the Indian Ocean to enter China exclusively through the Hengduan Mountains. This has brought abundant rainfall to the southeastern Tibetan Plateau, significantly impacting species in that region, such as *Cardiocrinum*, *Chamaesium thalictrifolium*, *Allium section Sikkimensia*, and *Rabdosia* (J. Li et al., 2022; C. Xie et al., 2019; X. Q. Yu et al., 2014; H. Y. Zheng et al., 2021). Our molecular dating analysis suggested that *N. thomsonianum* diverged during the late Miocene (7.43 Ma, 95% HPD: 14.86-2.53 Ma). Therefore, we infer that climate change and complex geological activity play important roles in the differentiation and dispersal of *Notholirion* species during this period.

During the Pleistocene period (2.588-0.126 Ma), the most far-reaching geological event was the Last Ice Age, a repeated cycle of alternating ice ages and interglacials that caused widespread climatic upheaval with unprecedented effects on the biology of the period (G. M. Hewitt, 2004). During the Ice Age, a continuous ice cap did not form on the Tibetan Plateau and surrounding areas, especially in the Hengduan Mountains located on *ITS* eastern edge. Intense orogenic movements in the Hengduan Mountains during and after the late Miocene caused the mountains to stretch north and south, resulting in high mountain valleys and diverse topography characterized by folded mountains and faulted basins. While the ice age caused most of the region to become cold and dry, there were still relatively warm and moist areas in the Hengduan Mountains region where organisms could survive. The harsh conditions of the ice age forced organisms to seek refuge in these areas, resulting in natural isolation that may have led to the divergence and formation of new species (Q. Meng et al., 2022). Through BEAST analysis, we discovered that the divergence of *N. macrophyllum* and *N. bulbuliferum* occurred during the Last Glacial Maximum (2.46 Ma, 95% HPD: 4.74-0.81 Ma), indicating that the significant climate fluctuations and natural isolation between different refuges may play a crucial role in the formation and distribution of these species.

4.4 Population dynamics history within *Notholirion*

The Quaternary Ice Age has been a highly significant and widely studied event in the field of biogeography. The climatic upheavals associated with this ice age, along with interglacial cycles, have had a profound impact on species ranges, often leading to population migration and even extinction (G. M. Hewitt, 2004). Based on our previous research on divergence timing, we have found that among the three species in the *Notholirion*, *N. thomsonianum* diverged as the early branch during the late Miocene, whereas the other two species did not fully diverge until the LGM period. Therefore, we speculate that the climatic fluctuations during the Quaternary Ice Age, particularly the significant temperature drop during the LGM, played a crucial role in shaping the range of the ancestral taxa of the *Notholirion* genus. These changes likely in turn contributed to the divergence of *N. bulbuliferum* and *N. macrophyllum*, leading to the formation of distinct species. According to the results predicted by our distribution models for the three periods (LIG, LGM and present), the suitable distribution area of *Notholirion* in the eastern part of the Tibetan Plateau contracted significantly toward *ITS* eastern edge during the Last Glacial Maximum (LGM), and then re-expanded toward the eastern part of the Plateau to *ITS* present distribution pattern after the LGM. Additionally, our mismatch distribution analysis based on both *ITS* and cpDNA data exhibited non-smooth bimodal or multi-peak curves (Figure). This, coupled with the non-star-like phylogeographical structure of haplotypes and non-significant results of the neutrality test, suggests that *Notholirion* had not recently undergone rapid expansion events (Figure, Table). We propose that the stability of *Notholirion* in *ITS* overall distribution range, as well as the observed contraction and re-expansion in the eastern Tibetan Plateau, can be attributed to *ITS* distinctive characteristics as an autochthonous high-altitude taxon, along with the combined influence of external environmental factors. These findings also indicate that the response of plant taxa across the eastern Tibetan Plateau and the Hengduan Mountains to Quaternary ice age climate change is more intricate and nuanced than previously assumed.

Numerous studies have provided evidence that during the Quaternary period, there was no uniform ice cap covering both the Tibetan Plateau and the Hengduan Mountains (G. M. Hewitt, 2004; Taberlet, Fumagalli, Wust-Saucy, & Cosson, 1998). Additionally, *Notholirion*, as a high-altitude plant taxon primarily found at elevations around 3000 m, exhibited enhanced cold and frost tolerance and a greater capacity to adapt to

the environmental fluctuations of the ice age. Consequently, it is plausible that certain widely distributed and cold-tolerant plant taxa, such as *Chamaesium*, *Allium* section *Sikkimensia*, and *Cardiocrinum*, including *Notholirion*, survived the ice age by persisting in multiple refugia and subsequently expanded their distribution following the ice age (J. Li et al., 2022; C. Xie et al., 2019; H. Y. Zheng et al., 2021). Furthermore, we observed notable levels of genetic diversity ($ITS : HD > 0.7$) and unique haplotypes specific in populations from BDY, BLQ, and BZD. In the context of genealogical geographic studies, regions exhibiting elevated genetic diversity or the presence of ancient and endemic haplotypes are often regarded as potential ice age refuges for plants (Tzedakis, Lawson, Frogley, Hewitt, & Preece, 2002). Based on these findings, we propose that the Hengduan Mountains and their neighboring areas could have served as refuges during the ice age for *Notholirion* species inhabiting both the eastern Tibetan Plateau and the Hengduan Mountains. Notably, this region has been recognized as a significant refuge for numerous plant taxa on the Tibetan Plateau, including *Potentilla glabra*, *Rhodiola alsia*, *Eriophyton wallichii*, and *Chamaesium* (Q. B. Gao et al., 2012; L. Y. Wang, Ikeda, Liu, Wang, & Liu, 2009; X. X. Wang, Yue, Sun, & Li, 2011; H. Y. Zheng et al., 2021). These findings suggest that the Quaternary ice age may have had less impact on the survival and widespread distribution of these high-elevation cold-tolerant plants in the subtropical region of the Tibetan Plateau than we thought. They survived on multiple ice-age refuges and rapidly regained their pre-glacial ranges after the ice age.

5 Conclusion

In conclusion, our study on the genetic diversity and structure of *Notholirion* sheds light on the intricate evolutionary history and adaptive mechanisms of this genus. The observed high genetic diversity of *Notholirion*, surpassing the average of angiosperms, is attributed to *ITS* early divergence in the late Oligocene and *ITS* adaptation to diverse climatic and geological events during *ITS* evolution. The unique "sky island" environments, resulting from complex topography in the Himalayan-Hengduan Mountains, contribute to the isolation of populations and, consequently, high genetic differentiation. The AMOVA analyses revealed substantial genetic variation among *Notholirion* populations, indicating limited communication between populations due to specific habitat requirements, restricted seed dispersal, and environmental factors influencing gene flow. This genetic differentiation is consistent with the impact of complex geological activities and climate changes in the Himalayan-Hengduan Mountains region. Phylogenetic analysis confirmed the monophyletic nature of *Notholirion*, with *N. thomsonianum* identified as the earliest divergent taxon. However, incongruences between nuclear and chloroplast gene trees suggest the influence of incomplete lineage sorting and hybridization, common phenomena in plant phylogenetics. The origin and diversification of *Notholirion* are closely tied to the uplift events on the Tibetan Plateau. The late Miocene and Pleistocene periods played pivotal roles in the evolution and distribution of *Notholirion* species, with significant climate fluctuations contributing to species divergence. The Last Glacial Maximum, in particular, led to the formation of distinct species, emphasizing the impact of Quaternary Ice Age climate changes on plant ranges and population dynamics. Our findings propose that *Notholirion*, as a high-altitude taxon, survived the ice age through persistence in multiple refugia, particularly in the Hengduan Mountains region. The study challenges previous assumptions about the uniformity of ice cap coverage in the Tibetan Plateau and Hengduan Mountains during the Quaternary period, suggesting a more nuanced response of cold-tolerant plant taxa to climate changes. Overall, this research contributes valuable insights into the evolutionary and ecological dynamics of *Notholirion*, highlighting the importance of considering multiple factors, including geological events, climatic changes, and specific ecological, in understanding the genetic diversity and adaptive strategies of high-altitude plant taxa.

Acknowledgments

This work was supported by the National Natural Science Foundation of China (Grant Nos. 32100180, 32070221, 32170209), and Survey on the Background Resources of Chengdu Area of Giant Panda National Park (Project No. 510101202200376).

Author contribution statement

Rui-Yu Cheng: Conceptualization, Formal analysis, Investigation, Methodology, Writing—original draft. Juan Li: Conceptualization, Investigation, Data curation, Formal analysis. Deng-Feng Xie: Formal analysis, Investigation, Methodology. Ren-Xiu Zhou: Formal analysis, Investigation. Qing Li: Funding acquisition. Yanglina Yu: Funding acquisition. Xing-Jin He: Investigation, Validation, Writing—review & editing. Song-Dong Zhou: Investigation, Validation, Writing—review & editing.

Declaration of Interest Statement

The authors declare that they have no known competing financial interests or personal relationships that could have appeared to influence the work reported in this paper.

Data availability

The datasets presented in this study can be found in online repositories. The names of the repositories and accession number(s) can be found below: <https://www.ncbi.nlm.nih.gov/genbank/>, (chloroplast genomes) OR899315 - OR899324; (*ITS*) OR898935 - OR899150 and OR899157 - OR899194, (*matK*) OR914272 - OR914525; (*ndhA*) OR897910 - OR898163; (*ndhG-I*) OR914680 - OR914933; (*petB-D*) OR917093 - OR917346; (*petL-G*) OR917454 - OR917707.

Reference :

- Aitchison, J. C., & Ali, J. R. (2008). When and where did India and Asia collide? *Geol Bull China* (9).
- Alemu, W. G., & Wimberly, M. C. (2020). Evaluation of Remotely Sensed and Interpolated Environmental Datasets for Vector-Borne Disease Monitoring Using In Situ Observations Over the Amhara Region, Ethiopia. *Sensors (Basel)*, 20 (5). doi:10.3390/s20051316
- Bandelt, H. J., Forster, P., & Röhl, A. (1999). Median-joining networks for inferring intraspecific phylogenies. *Mol Biol Evol*, 16 (1), 37-48. doi:10.1093/oxfordjournals.molbev.a026036
- Borns, H. W. (1994). *The ice age world : an introduction to quaternary history and research with emphasis on North America and Northern Europe during the last 2.5 million years* : Scandinavian University Press.
- Buckley, T. R., Cordeiro, M., Marshall, D. C., & Simon, C. (2006). Differentiating between hypotheses of lineage sorting and introgression in New Zealand alpine cicadas (Maoricicada Dugdale). *Syst Biol*, 55 (3), 411-425. doi:10.1080/10635150600697283
- Buerki, S., Jose, S., Yadav, S. R., Goldblatt, P., Manning, J. C., & Forest, F. (2012). Contrasting biogeographic and diversification patterns in two Mediterranean-type ecosystems. *PLoS One*, 7 (6), e39377. doi:10.1371/journal.pone.0039377
- Cao, J. L., Shi, Y. L., Zhang, H., & Wang, H. (2009). Numerical simulation of GPS observed clockwise rotation around the eastern Himalayan syntax in the Tibetan Plateau. *Chin Sci Bull* .
- Chatterjee, S., Goswami, A., & Scotese, C. R. (2013). The longest voyage: Tectonic, magmatic, and paleoclimatic evolution of the Indian plate during its northward flight from Gondwana to Asia. *Gondwana Res*, 23 (1), 238-267.
- Chen, J. M., Zhi-Yuan, D. U., Yuan, Y. Y., & Wang, Q. F. (2014). Phylogeography of an alpine aquatic herb *Ranunculus bungei* (Ranunculaceae) on the Qinghai–Tibet Plateau. *J Syst Evol*, 52 (003), 313-325.
- Chen, S. C., Liang, S. J., Xu, J. M., & Minoru, N. T. (2000). Liliaceae A. L. Jussieu. *Flora of China*, 14 , 73-263.
- Deng, T. D., Tao., Ding, L. D., Lin., & Deng, T. (2015). Paleoaltimetry reconstructions of the Tibetan Plateau: progress and contradictions. *Natl Sci Rev*, 2 (4), 417-437.
- Dierckxsens, N., Mardulyn, P., & Smits, G. (2017). NOVOPlasty: de novo assembly of organelle genomes from whole genome data. *Nucleic Acids Res*, 45 (4), e18. doi:10.1093/nar/gkw955

- Douglas, N. A., Wall, W. A., Xiang, Q. Y., Hoffmann, W. A., Wentworth, T. R., Gray, J. B., & Hohmann, M. G. (2011). Recent vicariance and the origin of the rare, edaphically specialized Sandhills lily, *Lilium pyrophilum* (Liliaceae): evidence from phylogenetic and coalescent analyses. *Mol Ecol*, *20* (14), 2901-2915. doi:10.1111/j.1365-294X.2011.05151.x
- Dupont-Nivet, G., Lippert, P. C., Hinsbergen, D., Meijers, M., & Kapp, P. (2010). Paleolatitude and age of the Indo-Asia collision: Paleomagnetic constraints. *Geophys J Int*, *182* (3), 1189-1198.
- E., P., & C., G. (1980). A rapid DNA isolation procedure for small quantities of fresh leaf tissue. *Phytochemistry* (19), 11-13.
- Elith, J., & Leathwick, J. R. (2009). Species Distribution Models: Ecological Explanation and Prediction Across Space and Time. *Annu Rev Ecol Evol Syst*, *40* (1), 677-697.
- Ellis, C. J., Yahr, R., Belinchón, R., & Coppins, B. J. (2014). Archaeobotanical evidence for climate as a driver of ecological community change across the anthropocene boundary. *Glob Chang Biol*, *20* (7), 2211-2220. doi:10.1111/gcb.12548
- Excoffier, L., & Lischer, H. E. (2010). Arlequin suite ver 3.5: a new series of programs to perform population genetics analyses under Linux and Windows. *Mol Ecol Resour*, *10* (3), 564-567. doi:10.1111/j.1755-0998.2010.02847.x
- Favre, A., Päckert, M., Pauls, S. U., Jähmig, S. C., Uhl, D., Michalak, I., & Muellner-Riehl, A. N. (2015). The role of the uplift of the Qinghai-Tibetan Plateau for the evolution of Tibetan biotas. *Biol Rev Camb Philos Soc*, *90* (1), 236-253. doi:10.1111/brv.12107
- Fawcett, T. (2005). An introduction to ROC analysis. *Pattern Recognit Lett*, *27* (8), 861-874.
- Fick, S. E., & Hijmans, R. J. (2017). WorldClim 2: New 1-km spatial resolution climate surfaces for global land areas. *Int J Climatol*, *37* (12).
- Fielding, A. (1997). A review of methods for the assessment of prediction errors in conservation presence/absence models. *Environ Conser*, *24* (1), 38-49.
- Gao, Q. B., Zhang, D. J., Duan, Y. Z., Zhang, F. Q., Yinhu, L. I., Pengcheng, F. U., & Chen, S. L. (2012). Intraspecific divergences of *Rhodiola alsia* (Crassulaceae) based on plastid DNA and internal transcribed spacer fragments. *BIOL J LINN SOC* .
- Gao, Y., Harris, A. J., Li, H., & Gao, X. (2020). Hybrid Speciation and Introgression Both Underlie the Genetic Structures and Evolutionary Relationships of Three Morphologically Distinct Species of *Lilium* (Liliaceae) Forming a Hybrid Zone Along an Elevational Gradient. *Front Plant Sci*, *11* , 576407. doi:10.3389/fpls.2020.576407
- Gao, Y. D., Harris, A. J., & He, X. J. (2015). Morphological and ecological divergence of *Lilium* and *Nomocharis* within the Hengduan Mountains and Qinghai-Tibetan Plateau may result from habitat specialization and hybridization. *BMC Evol Biol*, *15* , 147. doi:10.1186/s12862-015-0405-2
- Gao, Y. D., Harris, A. J., Zhou, S. D., & He, X. J. (2013). Evolutionary events in *Lilium* (including *Nomocharis*, Liliaceae) are temporally correlated with orogenies of the Q-T plateau and the Hengduan Mountains. *Mol Phylogenet Evol*, *68* (3), 443-460. doi:10.1016/j.ympev.2013.04.026
- Gernhard, T. (2008). The conditioned reconstructed process. *J Theor Biol*, *253* (4), 769-778. doi:10.1016/j.jtbi.2008.04.005
- Helfrich, P., Rieb, E., Abrami, G., Lücking, A., & Mehler, A. (2018). *TreeAnnotator: versatile visual annotation of hierarchical text relations*. Paper presented at the Proceedings of the eleventh international conference on language resources and evaluation (LREC 2018).

- Hewitt, G. (2000). The genetic legacy of the Quaternary ice ages. *Nature*, *405* (6789), 907-913. doi:10.1038/35016000
- Hewitt, G. M. (1996). Some genetic consequences of ice ages, and their role in divergence and speciation. *BIOL J LINN SOC* (3), 247-276.
- Hewitt, G. M. (2004). Genetic consequences of climatic oscillations in the Quaternary. *Philos Trans R Soc Lond B Biol Sci*, *359* (1442), 183-195; discussion 195. doi:10.1098/rstb.2003.1388
- Hickerson, M. J., Carstens, B. C., Cavender-Bares, J., Crandall, K. A., Graham, C. H., Johnson, J. B., . . . Yoder, A. D. (2010). Phylogeography's past, present, and future: 10 years after Avise, 2000. *Mol Phylogenet Evol*, *54* (1), 291-301. doi:10.1016/j.ympev.2009.09.016
- Hijmans, R. J., Cameron, S. E., Parra, J. L., Jones, P. G., & Jarvis, A. (2010). Very high resolution interpolated climate surfaces for global land areas. *Int J Climatol*, *25* (15), 1965-1978.
- Huang, J., Yang, L. Q., Yu, Y., Liu, Y. M., Xie, D. F., Li, J., . . . Zhou, S. D. (2018). Molecular phylogenetics and historical biogeography of the tribe Liliae (Liliaceae): bi-directional dispersal between biodiversity hotspots in Eurasia. *Ann Bot*, *122* (7), 1245-1262. doi:10.1093/aob/mcy138
- Huntington, K. W., Blythe, A. E., & Hodges, K. V. (2006). Climate change and Late Pliocene acceleration of erosion in the Himalaya. *Earth Planet Sci Lett*, *252* (1-2), 107-118.
- Kai, H., & Jiang, X. (2014). Sky islands of southwest China. I: An overview of phylogeographic patterns. *Chin Sci Bull*, *59* (7), 1-13.
- Kalyanamoorthy, S., Minh, B. Q., Wong, T. K. F., von Haeseler, A., & Jermin, L. S. (2017). ModelFinder: fast model selection for accurate phylogenetic estimates. *Nat Methods*, *14* (6), 587-589. doi:10.1038/nmeth.4285
- Katoh, K., & Standley, D. M. (2013). MAFFT multiple sequence alignment software version 7: improvements in performance and usability. *Mol Biol Evol*, *30* (4), 772-780. doi:10.1093/molbev/mst010
- Kearse, M., Moir, R., Wilson, A., Stones-Havas, S., Cheung, M., Sturrock, S., . . . Drummond, A. (2012). Geneious Basic: an integrated and extendable desktop software platform for the organization and analysis of sequence data. *Bioinformatics*, *28* (12), 1647-1649. doi:10.1093/bioinformatics/bts199
- Keller, I., & Seehausen, O. (2012). Thermal adaptation and ecological speciation. *Mol Ecol*, *21* (4), 782-799. doi:10.1111/j.1365-294X.2011.05397.x
- Kim, J. S., & Kim, J. H. (2018). Updated molecular phylogenetic analysis, dating and biogeographical history of the lily family (Liliaceae: Liliales). *Bot. J. Linn. Soc.*, *187* (4), 579-593.
- Kumar, S., Stecher, G., Li, M., Knyaz, C., & Tamura, K. (2018). MEGA X: Molecular Evolutionary Genetics Analysis across Computing Platforms. *Mol Biol Evol*, *35* (6), 1547-1549. doi:10.1093/molbev/msy096
- Lanfear, R., Frandsen, P. B., Wright, A. M., Senfeld, T., & Calcott, B. (2017). PartitionFinder 2: New Methods for Selecting Partitioned Models of Evolution for Molecular and Morphological Phylogenetic Analyses. *Mol Biol Evol*, *34* (3), 772-773. doi:10.1093/molbev/msw260
- Les, D. H., Peredo, E. L., King, U. M., Benoit, L. K., Tippery, N. P., Ball, C. J., & Shannon, R. K. (2015). Through thick and thin: cryptic sympatric speciation in the submersed genus *Najas* (Hydrocharitaceae). *Mol Phylogenet Evol*, *82 Pt A*, 15-30. doi:10.1016/j.ympev.2014.09.022
- Li, D. Z. (2008). Floristics and plant biogeography in China. *J Integr Plant Biol*, *50* (7), 771-777. doi:10.1111/j.1744-7909.2008.00711.x
- Li, H. T., Yi, T. S., Gao, L. M., Ma, P. F., Zhang, T., Yang, J. B., . . . Li, D. Z. (2019). Origin of angiosperms and the puzzle of the Jurassic gap. *Nat Plants*, *5* (5), 461-470. doi:10.1038/s41477-019-0421-0

- Li, J., Cai, J., Qin, H. H., Price, M., Zhang, Z., Yu, Y., . . . Gao, X. F. (2022). Phylogeny, Age, and Evolution of Tribe Liliae (Liliaceae) Based on Whole Plastid Genomes. *Front Plant Sci*, *12*, 699226. doi:10.3389/fpls.2021.699226
- Li, J., Milne, R. I., Ru, D., Miao, J., Tao, W., Zhang, L., . . . Mao, K. (2020). Allopatric divergence and hybridization within *Cupressus chengiana* (Cupressaceae), a threatened conifer in the northern Hengduan Mountains of western China. *Mol Ecol*, *29* (7), 1250-1266. doi:10.1111/mec.15407
- Li, M. J., Yu, H. X., Guo, X. L., & He, X. J. (2021). Out of the Qinghai-Tibetan Plateau and rapid radiation across Eurasia for *Allium* section *Daghestanica* (Amaryllidaceae). *AoB Plants*, *13* (3), plab017. doi:10.1093/aobpla/plab017
- Li, Q., Guo, X., Niu, J., Duojie, D., Li, X., Opgenoorth, L., & Zou, J. (2020). Molecular Phylogeography and Evolutionary History of the Endemic Species *Corydalis hendersonii* (Papaveraceae) on the Tibetan Plateau Inferred From Chloroplast DNA and ITS Sequence Variation. *Front Plant Sci*, *11*, 436. doi:10.3389/fpls.2020.00436
- Liu, H. R., Khan, G., Gao, Q., Zhang, F., Liu, W., Wang, Y., . . . Afridi, S. G. (2022). Dispersal into the Qinghai-Tibet plateau: evidence from the genetic structure and demography of the alpine plant *Triosteum pinnatifidum*. *PeerJ*, *10*, e12754. doi:10.7717/peerj.12754
- Liu, J. Q., Duan, Y., Hao, G., XuemgUn, G., & Sun, H. (2014). Evolutionary history and underlying adaptation of alpine plants on the Qinghai-Tibet Plateau. *J Syst Evol*, *52* (3), 241-249.
- Liu, J. Q., Sun, Y. S., Ge, X. J., Gao, L. M., & Qiu, Y. X. (2012). Phylogeographic studies of plants in China: Advances in the past and directions in the future. *J Biogeogr*, *50* (3), 267-275.
- Liu, M. L., He, Y. L., Lopez-Pujol, J., Jia, Y., & Li, Z. H. (2019). Complex population evolutionary history of four cold-tolerant *Notopterygium* herb species in the Qinghai-Tibetan Plateau and adjacent areas. *Heredity (Edinb)*, *123* (2), 242-263. doi:10.1038/s41437-019-0186-2
- Liu, X., Wang, Z., Shao, W., Ye, Z., & Zhang, J. (2016). Phylogenetic and Taxonomic Status Analyses of the Abaso Section from Multiple Nuclear Genes and Plastid Fragments Reveal New Insights into the North America Origin of *Populus* (Salicaceae). *Front Plant Sci*, *7*, 2022. doi:10.3389/fpls.2016.02022
- Luo, D., Yue, J. P., & Sun, W. G. (2016). Evolutionary history of the subnival flora of the Himalaya-Hengduan Mountains: first insights from comparative phylogeography of four perennial herbs. *J Biogeogr*.
- Maddison, W. P. (1997). Gene trees in species trees. *Syst. Biol.*, *46* (3), 523-536.
- Marchese, C. (2015). Biodiversity hotspots: A shortcut for a more complicated concept. *Glob Ecol Conserv*, *3* (74), 297-309.
- Meng, H. H., Su, T., Gao, X. Y., Li, J., Jiang, X. L., Sun, H., & Zhou, Z. K. (2017). Warm-cold colonization: response of oaks to uplift of the Himalaya-Hengduan Mountains. *Mol Ecol*, *26* (12), 3276-3294. doi:10.1111/mec.14092
- Meng, Q., Xie, Z., Xu, H., Guo, J., Tang, Y., Ma, T., . . . Gao, T. (2022). Out of the Qinghai-Tibetan plateau: Origin, evolution and historical biogeography of *Morchella* (both *Elata* and *Esculenta* clades). *Front Microbiol*, *13*, 1078663. doi:10.3389/fmicb.2022.1078663
- Mulch, A., & Chamberlain, C. P. (2006). Earth science: the rise and growth of Tibet. *Nature*, *439* (7077), 670-671. doi:10.1038/439670a
- Muratović, E., Robin, O., Bogunić, F., Šoljan, D., & Siljak-Yakovlev, S. (2010). Karyotype evolution and speciation of European lilies from *Lilium* sect. *Liriotypus*. *Taxon*, *59* (1), 165-175.

- Nei, M., & Li, W. H. (1979). Mathematical model for studying genetic variation in terms of restriction endonucleases. *Proc Natl Acad Sci U S A*, *76* (10), 5269-5273. doi:10.1073/pnas.76.10.5269
- Nei, M., & Tajima, F. (1981). DNA polymorphism detectable by restriction endonucleases. *Genetics*, *97* (1), 145-163. doi:10.1093/genetics/97.1.145
- Nge, F. J., Biffin, E., Thiele, K. R., & Waycott, M. (2020). Extinction pulse at Eocene-Oligocene boundary drives diversification dynamics of two Australian temperate floras. *Proc Biol Sci*, *287* (1919), 20192546. doi:10.1098/rspb.2019.2546
- Ni, L., Li, W., Zhao, Z., Gaawe, D., & Liu, T. (2022). Migration patterns of *Gentiana crassicaulis*, an alpine gentian endemic to the Himalaya-Hengduan Mountains. *Ecol Evol*, *12* (3), e8703. doi:10.1002/ece3.8703
- O'Brien, C. L., Huber, M., Thomas, E., Pagani, M., Super, J. R., Elder, L. E., & Hull, P. M. (2020). The enigma of Oligocene climate and global surface temperature evolution. *Proc Natl Acad Sci U S A*, *117* (41), 25302-25309. doi:10.1073/pnas.2003914117
- Pelkonen, V. P., Niittyvuopio, A., Pirttilä, A. M., Laine, K., & Hohtola, A. (2007). Phylogenetic background of Orange lily (*Lilium bulbiferum* s.l.) cultivars from a genetically isolated environment. *Plant Biol (Stuttg)*, *9* (4), 534-540. doi:10.1055/s-2007-965042
- Pelser, P. B., Kennedy, A. H., Tepe, E. J., Shidler, J. B., Nordenstam, B., Kadereit, J. W., & Watson, L. E. (2010). Patterns and causes of incongruence between plastid and nuclear Senecioneae (Asteraceae) phylogenies. *Am J Bot*, *97* (5), 856-873. doi:10.3732/ajb.0900287
- Peterson, A. T., Pape, M., & Soberón, J. (2008). Rethinking receiver operating characteristic analysis applications in ecological niche modeling. *Ecol Modell* (1).
- Petit, R. J., Duminil, J., Fineschi, S., Hampe, A., Salvini, D., & Vendramin, G. G. (2005). Comparative organization of chloroplast, mitochondrial and nuclear diversity in plant populations. *Mol Ecol*, *14* (3), 689-701. doi:10.1111/j.1365-294X.2004.02410.x
- Phillips, S. J., Anderson, R. P., & Schapire, R. E. (2006). Maximum entropy modeling of species geographic distributions. *Ecol Modell*, *190* (3-4), 231-259.
- Pons, O., & Petit, R. J. (1996). Measuring and testing genetic differentiation with ordered versus unordered alleles. *Genetics*, *144* (3), 1237-1245. doi:10.1093/genetics/144.3.1237
- Qian, H., Ricklefs, R. E., & Thuiller, W. (2021). Evolutionary assembly of flowering plants into sky islands. *Nat Ecol Evol*, *5* (5), 640-646. doi:10.1038/s41559-021-01423-1
- Qiu, Y. X., Fu, C. X., & Comes, H. P. (2011). Plant molecular phylogeography in China and adjacent regions: Tracing the genetic imprints of Quaternary climate and environmental change in the world's most diverse temperate flora. *Mol Phylogenet Evol*, *59* (1), 225-244. doi:10.1016/j.ympev.2011.01.012
- Qu, X. J., Moore, M. J., Li, D. Z., & Yi, T. S. (2019). PGA: a software package for rapid, accurate, and flexible batch annotation of plastomes. *Plant Methods*, *15* (1), 1-12. doi:10.1186/s13007-019-0435-7
- Rambaut, A. (2014). FigTree: a graphical viewer of phylogenetic trees, version 1.4. 2. *Institute of Evolutionary Biology, Univ. Edinburgh*.
- Ronquist, F., Teslenko, M., van der Mark, P., Ayres, D. L., Darling, A., Höhna, S., . . . Huelsenbeck, J. P. (2012). MrBayes 3.2: efficient Bayesian phylogenetic inference and model choice across a large model space. *Syst Biol*, *61* (3), 539-542. doi:10.1093/sysbio/sys029
- Rozas, J., Ferrer-Mata, A., Sánchez-DelBarrio, J. C., Guirao-Rico, S., Librado, P., Ramos-Onsins, S. E., & Sánchez-Gracia, A. (2017). DnaSP 6: DNA Sequence Polymorphism Analysis of Large Data Sets. *Mol Biol Evol*, *34* (12), 3299-3302. doi:10.1093/molbev/msx248

- Saylor, J. E., Quade, J., Dettman, D. L., Decelles, P. G., Kapp, P. A., & Ding, L. (2009). The late Miocene through present paleoelevation history of southwestern Tibet. *Am J Sci*, *309* (1), 1-42.
- Schneider, S., & Excoffier, L. (1999). Estimation of past demographic parameters from the distribution of pairwise differences when the mutation rates vary among sites: application to human mitochondrial DNA. *Genetics*, *152* (3), 1079-1089. doi:10.1093/genetics/152.3.1079
- Shahzad, K., Jia, Y., Chen, F. L., Zeb, U., & Li, Z. H. (2017). Effects of Mountain Uplift and Climatic Oscillations on Phylogeography and Species Divergence in Four Endangered Notopterygium Herbs. *Front Plant Sci*, *8*, 1929. doi:10.3389/fpls.2017.01929
- Soltis, P. S., & Soltis, D. E. (1991). Genetic Variation in Endemic and Widespread Plant Species. *Aliso*, *13* (1).
- Song, G., Zhang, R. Y., Qu, Y. H., Wang, Z. H., Dong, L., Kristin, A., . . . Lei, F. M. (2016). A zoogeographical boundary between the Palaearctic and Sino-Japanese realms documented by consistent north/south phylogeographical divergences in three woodland birds in eastern China. *J Biogeogr*, *43* (11).
- Stamatakis, A. (2014). RAxML version 8: a tool for phylogenetic analysis and post-analysis of large phylogenies. *Bioinformatics*, *30* (9), 1312-1313. doi:10.1093/bioinformatics/btu033
- Straume, E. O., Nummelin, A., Gaina, C., & Nisancioglu, K. H. (2022). Climate transition at the Eocene-Oligocene influenced by bathymetric changes to the Atlantic-Arctic oceanic gateways. *Proc Natl Acad Sci U S A*, *119* (17), e2115346119. doi:10.1073/pnas.2115346119
- Suchard, M. A., Lemey, P., Baele, G., Ayres, D. L., Drummond, A. J., & Rambaut, A. (2018). Bayesian phylogenetic and phylodynamic data integration using BEAST 1.10. *Virus Evol*, *4* (1), vey016. doi:10.1093/ve/vey016
- Sun, X., & Wang, P. (2005). How old is the Asian monsoon system? Paleobotanical records from China. *Paleogeogr Paleoclimatol Paleoecol*, *222* (3-4), 181-222.
- Sun, Y., Abbott, R. J., Li, L., Li, L., Zou, J., & Liu, J. (2014). Evolutionary history of Purple cone spruce (*Picea purpurea*) in the Qinghai-Tibet Plateau: homoploid hybrid origin and Pleistocene expansion. *Mol Ecol*, *23* (2), 343-359. doi:10.1111/mec.12599
- Taberlet, P., Fumagalli, L., Wust-Saucy, A. G., & Cosson, J. F. (1998). Comparative phylogeography and postglacial colonization routes in Europe. *Mol. Ecol*, *7* (4), 453-464.
- Tajima, F. (1989). Statistical method for testing the neutral mutation hypothesis by DNA polymorphism. *Genetics*, *123* (3), 585-595. doi:10.1093/genetics/123.3.585
- Tu, T., Volis, S., Dillon, M. O., Sun, H., & Wen, J. (2010). Dispersals of Hyoscyameae and Mandragoreae (Solanaceae) from the New World to Eurasia in the early Miocene and their biogeographic diversification within Eurasia. *Mol Phylogenet Evol*, *57* (3), 1226-1237. doi:10.1016/j.ympev.2010.09.007
- Tzedakis, P. C., Lawson, I. T., Frogley, M. R., Hewitt, G. M., & Preece, R. C. (2002). Buffered tree population changes in a Quaternary refugium: evolutionary implications. *Science*, *297* (5589), 2044-2047.
- Vranckx, G., Jacquemyn, H., Muys, B., & Honnay, O. (2012). Meta-analysis of susceptibility of woody plants to loss of genetic diversity through habitat fragmentation. *Conserv Biol*, *26* (2), 228-237. doi:10.1111/j.1523-1739.2011.01778.x
- Wang, H., Laqiong, Sun, K., Lu, F., Wang, Y., Song, Z., . . . Zhang, W. (2010). Phylogeographic structure of *Hippophae tibetana* (Elaeagnaceae) highlights the highest microrefugia and the rapid uplift of the Qinghai-Tibetan Plateau. *Mol Ecol*, *19* (14), 2964-2979. doi:10.1111/j.1365-294X.2010.04729.x
- Wang, L., Yang, W., Zhang, X., Zhang, D., & Zhang, G. (2023). Insights into the evolutionary history and taxonomic status of *Sinopteris* (Pteridaceae). *Mol Phylogenet Evol*, *180*, 107672.

doi:10.1016/j.ympev.2022.107672

Wang, L. Y., Ikeda, H., Liu, T. L., Wang, Y. J., & Liu, J. Q. (2009). Repeated range expansion and glacial endurance of *Potentilla glabra* (Rosaceae) in the Qinghai-Tibetan plateau. *J Integr Plant Biol*, *51* (7), 698-706. doi:10.1111/j.1744-7909.2009.00818.x

Wang, X. X., Yue, J. P., Sun, H., & Li, Z. M. (2011). Phylogeographical study on *Eriophyton wallichii* (Labiatae) from alpine scree of Qinghai-Tibetan Plateau. *Plant Divers. Resour.*, *33* (6), 605-614.

White, T. J., Bruns, S., Lee, S., & Taylor, J. (1990). Amplification and direct sequencing of fungal ribosomal RNA genes for phylogenetics. *Trends Biochem Sci* (1), 315-322. doi: 10.1016/B978-0-12-372180-8.50042-1

Xia, M., Liu, Y., Liu, J., Chen, D., Shi, Y., Chen, Z., . . . Qiu, Y. (2022). Out of the Himalaya-Hengduan Mountains: Phylogenomics, biogeography and diversification of *Polygonatum* Mill. (Asparagaceae) in the Northern Hemisphere. *Mol Phylogenet Evol*, *169* , 107431. doi:10.1016/j.ympev.2022.107431

Xie, C., Xie, D. F., Zhong, Y., Guo, X. L., Liu, Q., Zhou, S. D., & He, X. J. (2019). The effect of Hengduan Mountains Region (HMR) uplift to environmental changes in the HMR and its eastern adjacent area: Tracing the evolutionary history of *Allium* section *Sikkimensia* (Amaryllidaceae). *Mol Phylogenet Evol*, *130* , 380-396. doi:10.1016/j.ympev.2018.09.011

Xie, D. F., Tan, J. B., Yu, Y., Gui, L. J., Su, D. M., Zhou, S. D., & He, X. J. (2020). Insights into phylogeny, age and evolution of *Allium* (Amaryllidaceae) based on the whole plastome sequences. *Ann Bot*, *125* (7), 1039-1055. doi:10.1093/aob/mcaa024

Xiong, Z., Liu, X., Ding, L., Farnsworth, A., Spicer, R. A., Xu, Q., . . . Yue, Y. (2022). The rise and demise of the Paleogene Central Tibetan Valley. *Sci Adv*, *8* (6), eabj0944. doi:10.1126/sciadv.abj0944

Xu, T., Abbott, R. J., Milne, R. I., Mao, K., Du, F. K., Wu, G., . . . Liu, J. (2010). Phylogeography and allopatric divergence of cypress species (*Cupressus* L.) in the Qinghai-Tibetan Plateau and adjacent regions. *BMC Evol Biol*, *10* , 194. doi:10.1186/1471-2148-10-194

Yang, F. S., Qin, A. L., Li, Y. F., & Wang, X. Q. (2012). Great genetic differentiation among populations of *Meconopsis integrifolia* and its implication for plant speciation in the Qinghai-Tibetan Plateau. *PLoS One*, *7* (5), e37196. doi:10.1371/journal.pone.0037196

Yang, J., Zhou, S., Huang, D., & He, X. (2018). Phylogeography of two closely related species of *Allium* endemic to East Asia: Population evolution in response to climate oscillations. *Ecol Evol*, *8* (16), 7986-7999. doi:10.1002/ece3.4338

Yang, M., Zhou, S., Xingjin, H. E., & Peng, C. (2016). Genetic Relationships of *Notholirion* and Genetic Diversity of *N. bulbiferum* in China Revealed by ISSR Markers. *Acta Botanica Boreali-Occidentalia Sinica* .

Yu, X. Q., Maki, M., Drew, B. T., Paton, A. J., Li, H. W., Zhao, J. L., . . . Li, J. (2014). Phylogeny and historical biogeography of *Isodon* (Lamiaceae): rapid radiation in south-west China and Miocene overland dispersal into Africa. *Mol Phylogenet Evol*, *77* , 183-194. doi:10.1016/j.ympev.2014.04.017

Yu, Y., Blair, C., & He, X. (2020). RASP 4: Ancestral State Reconstruction Tool for Multiple Genes and Characters. *Mol Biol Evol*, *37* (2), 604-606. doi:10.1093/molbev/msz257

Yu, Y., Harris, A. J., Blair, C., & He, X. (2015). RASP (Reconstruct Ancestral State in Phylogenies): a tool for historical biogeography. *Mol Phylogenet Evol*, *87* , 46-49. doi:10.1016/j.ympev.2015.03.008

Zhang, D., Gao, F., Jakovlić, I., Zou, H., Zhang, J., Li, W. X., & Wang, G. T. (2020). PhyloSuite: An integrated and scalable desktop platform for streamlined molecular sequence data management and evolutionary phylogenetics studies. *Mol Ecol Resour*, *20* (1), 348-355. doi:10.1111/1755-0998.13096

Zhang, P. Z., Shen, Z., Min, W., Gan, W., Bürgmann, R., Molnar, P., . . . Wu, J. (2004). Continuous deformation of the Tibetan Plateau from global positioning system data. *Geology*, *32* (9), 809-812.

Zhang, Q., & Willems, H. (2012). Initial India-Asia Continental Collision and Foreland Basin Evolution in the Tethyan Himalaya of Tibet: Evidence from Stratigraphy and Paleontology. *J Geol*, *120* (3), 347-347.

Zhang, Y. L., Li, B. Y., & Zheng, D. (2002). A discussion on the boundary and area of the Tibetan Plateau in China. *Geogr Res*, *21* (001), 1-8.

Zhang, Z., & Sun, J. (2011). Palynological evidence for Neogene environmental change in the foreland basin of the southern Tianshan range, northwestern China. *Glob Planet Change*, *75* (1-2), 56-66.

Zheng, H. B., Powell, C. M., An, Z. S., Zhou, J., & Dong, G. R. (2000). Pliocene uplift of the northern Tibetan Plateau. *Geology*, *28* (8), 715.

Zheng, H. Y., Guo, X. L., Price, M., He, X. J., & Zhou, S. D. (2021). Effects of Mountain Uplift and Climatic Oscillations on Phylogeography and Species Divergence of *Chamaesium* (Apiaceae). *Front Plant Sci*, *12* , 673200. doi:10.3389/fpls.2021.673200

Figure legends

Fig. 1 Sampling locations of *Notholirion*.

Fig. 2 Geographic distribution of *ITS* haplotypes for *Notholirion*. Circles represent populations and the colored outlines of the distinguish different species. Each color represents a haplotype.

Fig. 3 Haplotypes network based on *ITS* within *Notholirion*. Each color represents a specie. The size of circles in the network corresponds to the frequency of each haplotype. The horizontal bars on the horizontal lines between different haplotypes represent the number of variant sites. Small solid black circles denoted hypothetical unsampled or extinct ancestral haplotypes.

Fig. 4 Geographic distribution of cpDNA haplotypes for *Notholirion*. Each circle represents a population and the colored outlines of the distinguish different species. Each color represents a haplotype.

Fig. 5 Haplotypes network based on cpDNA within *Notholirion*. Each color represents a specie.

The size of circles in the network corresponds to the frequency of each haplotype. The horizontal bars on the horizontal lines between different haplotypes represent the number of variant sites. Small solid black circles denoted hypothetical unsampled or extinct ancestral haplotypes.

Fig. 6 Phylogenetic relationship of *Notholirion* recovered from the (a) *ITS* haplotypes and (b) chloroplast haplotypes. Bule clades: *N. bulbuliferum* , yellow clades: *N. macrophyllum* , red purple clades: *N. thomsonianum* . Maximum-likelihood bootstrap support/Bayesian posterior probability values are shown near corresponding nodes (‘-’ indicates support values less than 50%; ‘*’ represents 100%/1 support).

Fig. 7 Chronogram of *Notholirion* from the phylogenetic relationship of Liliales based on plastomes. The red boxes show species of the *Notholirion* .

Fig. 8 Divergence time estimation based on plastomes of *Notholirion*. Blue bars and numbers above represent 95% highest posterior density (95% HPDs) for each node.

Fig. 9 Ancestral area reconstructions based on the cpDNA phylogeny within *Notholirion*. Pie charts show proportions of the ancestral ranges. The map shows the three geographical distribution areas of *Notholirion* : (A) Southern Himalayas, (B) Eastern Himalayas, (C) Hengduan Mountains. The divergence time (in Ma) based on cpDNA. Numbers in the brackets show the 95% HPD of divergence time (in Ma) of the main nodes.

Fig. 10 Mismatch distribution analysis for *ITS* data (a) and cpDNA data (b). The line represents the distributions of an expected population expansion, the dashed line show observed (Obs) values.

Fig. 11 Potential distribution ranges of different periods for *Notholirion* were simulated by Species Distribution Models using Bioclimatic variables. Colors represent bioclimatic suitability, from most suitable (red) to unsuitable (gray). LIG: Last Interglacial, LGM: Last Glacial Maximum.

Supporting information

Table S1 The information of sample collection and geographical area for *Notholirion* .

Table S2 The genbank accessions for species used in differentiation time estimates.

Table S3 Priors and mean ages used to calibrate the Liliales phylogenomic tree.

Table S4 The haplotype distribution, haplotype diversity (Hd) and nucleotide diversity (Pi) in each population within *Notholirion* .

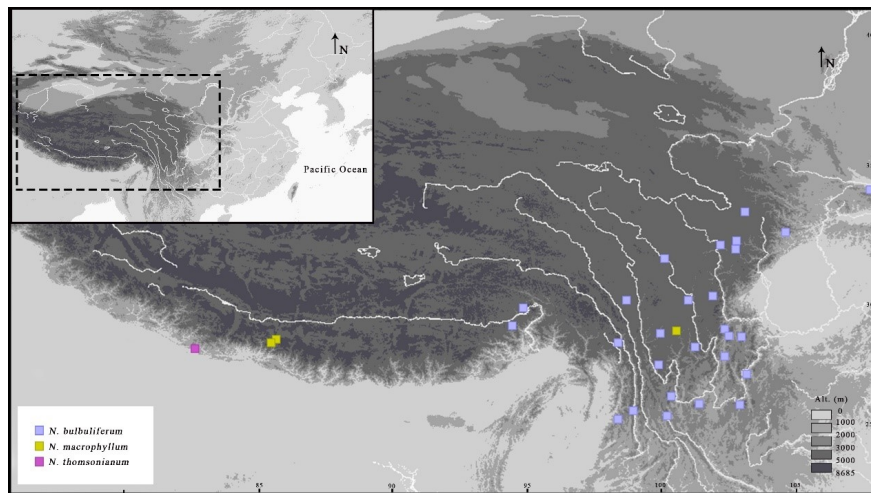


Figure 1: Sampling locations of *Notholirion*

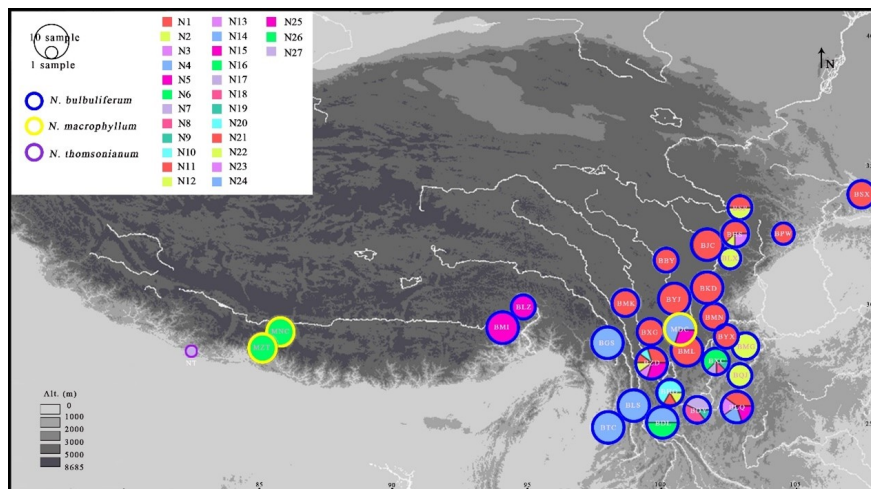


Figure 2: Geographic distribution of ITS haplotypes for *Notholirion*.

Circles represent populations and the colored outlines of the distinguish different species. Each color represents a haplotype.

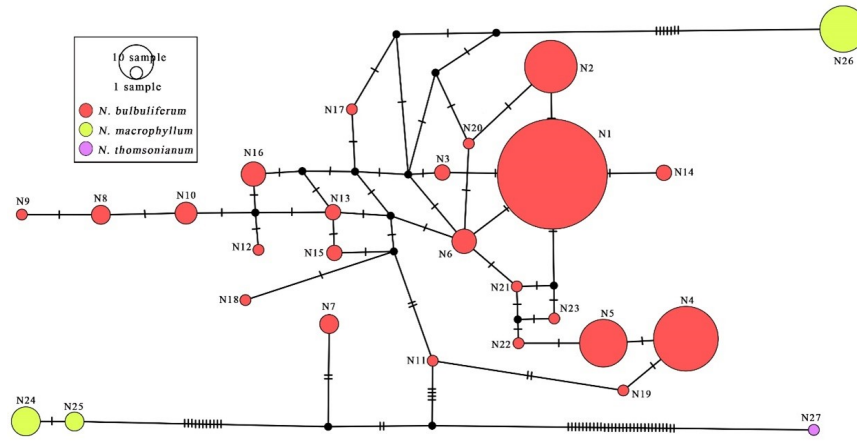


Figure 3: Haplotypes network based on ITS within *Notholirion*.

Each color represents a specie. The size of circles in the network corresponds to the frequency of each haplotype. The horizontal bars on the horizontal lines between different haplotypes represent the number of variant sites. Small solid black circles denoted hypothetical unsampled or extinct ancestral haplotypes.

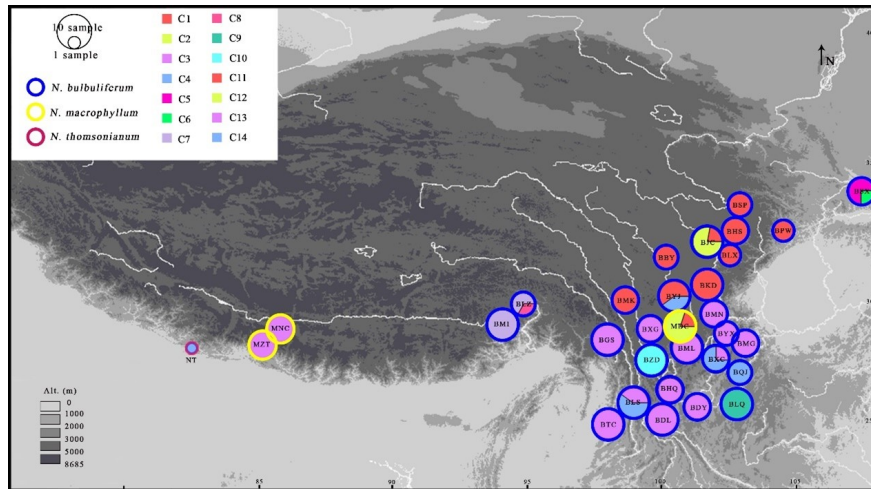


Figure 4: Geographic distribution of cpDNA haplotypes for *Notholirion*.

Each circle represents a population and the colored outlines of the distinguish different species. Each color represents a haplotype.

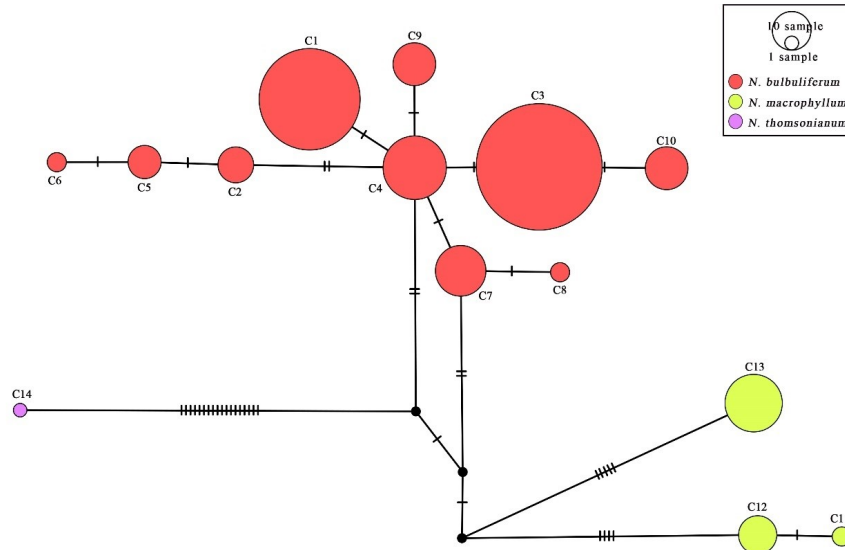


Figure 5: Haplotypes network based on cpDNA within *Notholirion*.

Each color represents a specie. The size of circles in the network corresponds to the frequency of each haplotype. The horizontal bars on the horizontal lines between different haplotypes represent the number of variant sites. Small solid black circles denoted hypothetical unsampled or extinct ancestral haplotypes.

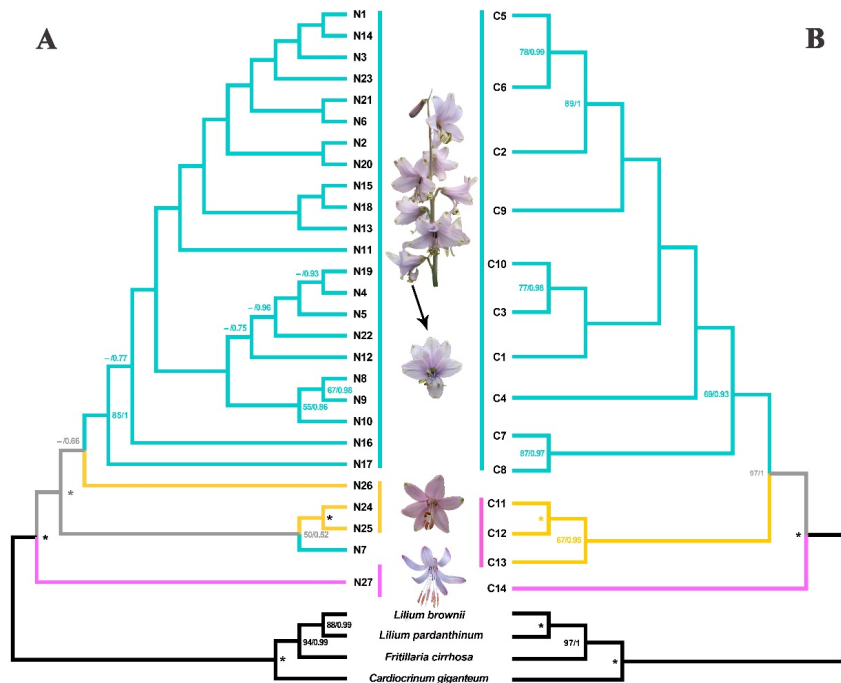


Figure 6: Phylogenetic relationship of *Notholirion* recovered from the (A) ITS haplotypes and (B) chloroplast haplotypes.

Blue clades: *N. bulbiferum* , yellow clades: *N. macrophyllum* , red purple clades: *N. thomsonianum* .
Maximum-likelihood bootstrap support/Bayesian posterior probability values are shown near corresponding nodes ('-' indicates support values less than 50%; '*' represents 100%/1 support).

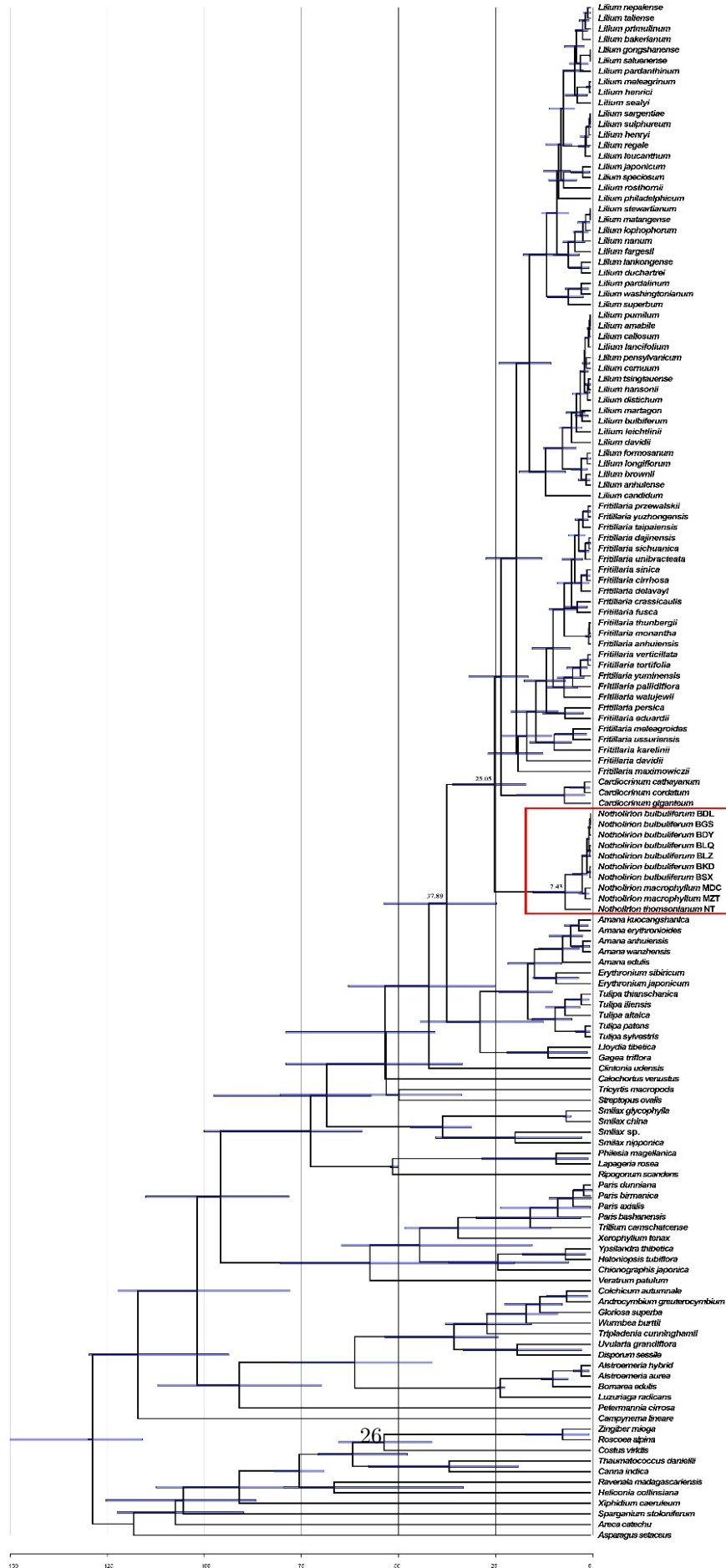


Figure 7: Chronogram of *Notholirion* from the phylogenetic relationship of Liliales based on plastomes.

The red boxes show species of the *Notholirion*.

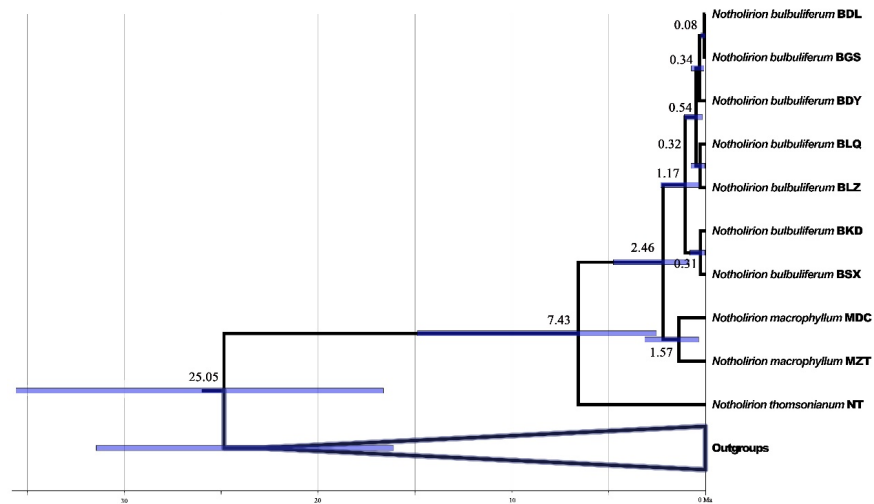


Figure 8: Divergence time estimation based on plastomes of *Notholirion*.

Blue bars and numbers above represent 95% highest posterior density (95% HPDs) for each node.

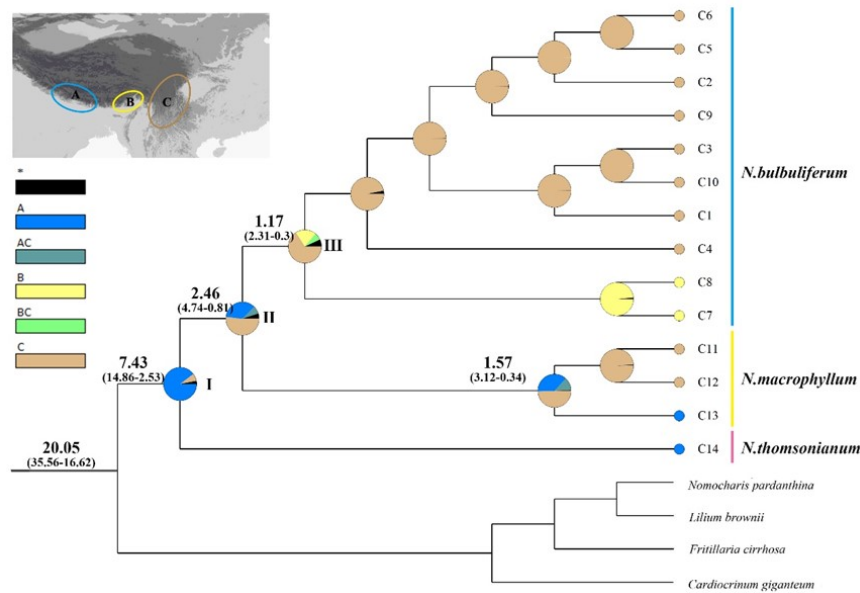


Figure 9: Ancestral area reconstructions based on the cpDNA phylogeny within *Notholirion*.

Pie charts show proportions of the ancestral ranges. The map shows the three geographical distribution areas of *Notholirion*: (A) Southern Himalayas, (B) Eastern Himalayas, (C) Hengduan Mountains. The divergence time (in Ma) based on cpDNA. Numbers in the brackets show the 95% HPD of divergence time (in Ma) of the main nodes.

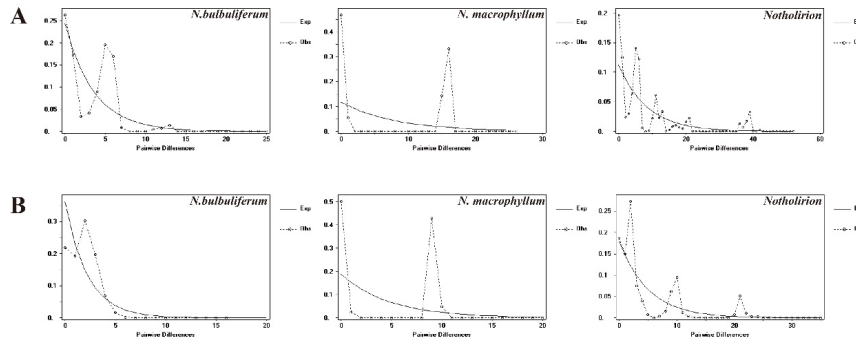


Figure 10: Mismatch distribution analysis for *ITS* data (A) and cpDNA data (B).

The line represents the distributions of an expected population expansion, the dashed line show observed (Obs) values.

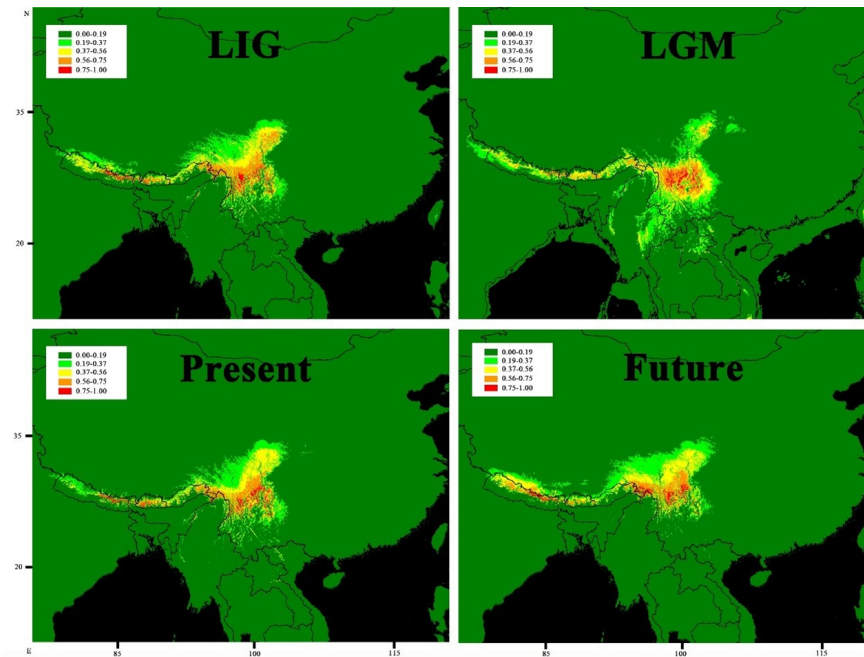


Figure 11: Potential distribution ranges of different periods for *Notholirion* were simulated by Species Distribution Models using Bioclimatic variables.

Colors represent bioclimatic suitability, from most suitable (red) to unsuitable (gray). LIG: Last Interglacial, LGM: Last Glacial Maximum.

Hosted file

Supplementary table1.docx available at <https://authorea.com/users/753582/articles/723781-effects-of-mountain-uplift-and-climatic-oscillations-on-phylogeography-and-species-divergence-of-notholirion-liliaceae>

Hosted file

Supplementary table2.docx available at <https://authorea.com/users/753582/articles/723781-effects-of-mountain-uplift-and-climatic-oscillations-on-phylogeography-and-species-divergence-of-notholirion-liliaceae>

Hosted file

Supplementary table3.docx available at <https://authorea.com/users/753582/articles/723781-effects-of-mountain-uplift-and-climatic-oscillations-on-phylogeography-and-species-divergence-of-notholirion-liliaceae>

Hosted file

Supplementary table4.docx available at <https://authorea.com/users/753582/articles/723781-effects-of-mountain-uplift-and-climatic-oscillations-on-phylogeography-and-species-divergence-of-notholirion-liliaceae>